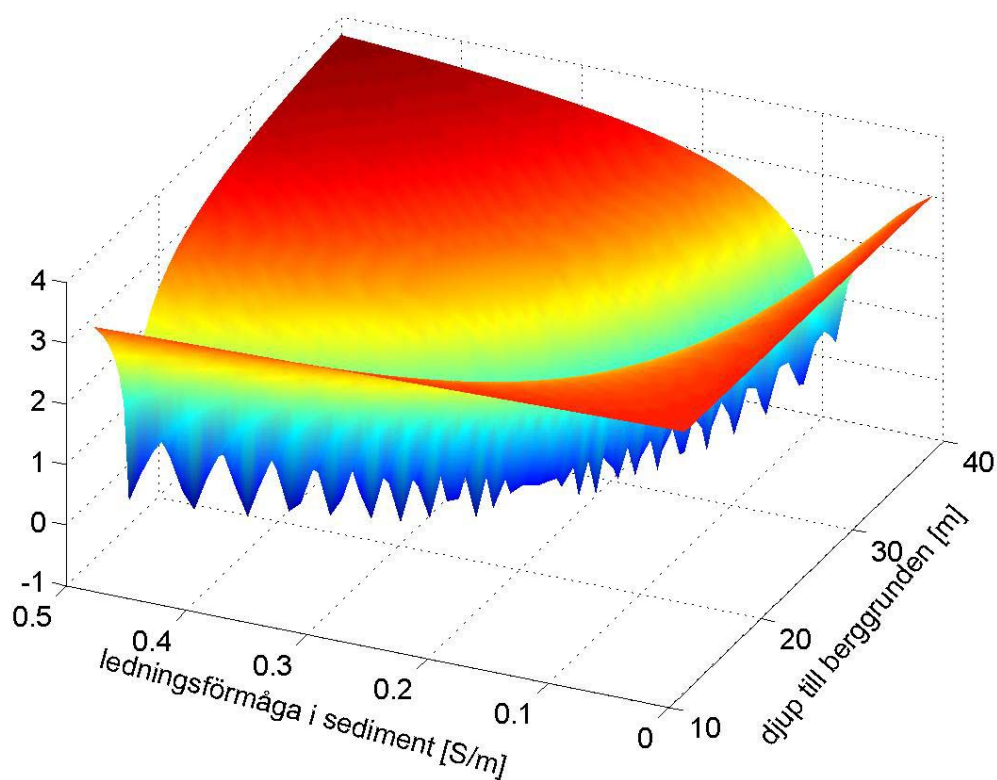


Jenny Schiöld

# Electromagnetic conductivity profile estimation by quasi-global restarting techniques of local Newton-like methods

Kostnadsfunktionen: Grunt vatten och sommarförhållanden



SWEDISH DEFENCE RESEARCH AGENCY

Systems Technology  
SE-172 90 Stockholm

FOI-R--0493--SE

June 2003

ISSN 1650-1942

**Technical report**

Jenny Schiöld

# Electromagnetic conductivity profile estimation by quasi-global restarting techniques of local Newton-like methods

<b>Issuing organization</b> FOI – Swedish Defence Research Agency Systems Technology SE-172 90 Stockholm	<b>Report number, ISRN</b> FOI-R--0493--SE	<b>Report type</b> Technical report
	<b>Research area code</b> 4. C4ISR	
	<b>Month year</b> May 2002	<b>Project no.</b> E6051
	<b>Customers code</b> 5. Commissioned Research	
	<b>Sub area code</b> 43 Underwater Sensors	
<b>Author/s (editor/s)</b> Jenny Schiöld	<b>Project manager</b> Peter Krylstedt	
	<b>Approved by</b> Monica Dahlén	
	<b>Sponsoring agency</b> Swedish Armed Forces	
	<b>Scientifically and technically responsible</b> Peter Krylstedt	
<b>Report title</b> Electromagnetic conductivity profile estimation by quasi-global restarting techniques of local Newton-like methods		
<b>Abstract (not more than 200 words)</b> <p>This report presents a multistart technique version of an inverse electromagnetic propagation computer program. The program calculates conductivities and layer depths in a horizontally stratified environment. The problem is formulated as a nonlinear least-squares problem, and to obtain a good solution a quasi-global optimisation technique is implemented. A local method is used combined with a multistart technique, so several solutions are obtained and the best solution may then be chosen. The program is then used to analyse some synthetic and some measured data.</p>		
<b>Keywords</b> inversion, REA, restarts		
<b>Further bibliographic information</b>	<b>Language</b> English	
<b>ISSN</b> 1650-1942	<b>Pages</b> 55 p.	
	<b>Price acc. to pricelist</b>	

<b>Utgivare</b> Totalförsvarets Forskningsinstitut - FOI Systemteknik 172 90 Stockholm	<b>Rapportnummer, ISRN</b> FOI-R--0493--SE	<b>Klassificering</b> Teknisk rapport
	<b>Forskningsområde</b> 4. Spaning och ledning	
	<b>Månad, år</b> Maj 2002	<b>Projektnummer</b> E6051
	<b>Verksamhetsgren</b> 5. Uppdragsfinansierad verksamhet	
	<b>Delområde</b> 43 Undervattenssensorer	
<b>Författare/redaktör</b> Jenny Schiöld	<b>Projektledare</b> Peter Krylstedt	
	<b>Godkänd av</b> Monica Dahlén	
	<b>Uppdragsgivare/kundbeteckning</b> Försvarsmakten	
	<b>Tekniskt och/eller vetenskapligt ansvarig</b> Peter Krylstedt	
<b>Rapportens titel (i översättning)</b> Elektromagnetisk konduktivitetsprofilestimering genom kvasi-globala återstartningstekniker av lokala Newton-lika metoder		
<b>Sammanfattning (högst 200 ord)</b> Rapporten presenterar en version av ett inverst elektromagnetiskt vågutbredningsprogram, som använder sig av en återstartningsteknik. Programmet beräknar konduktiviteter och lagertjocklekar hos ett godtyckligt antal lager i en horisontellt skiktad miljö. Problemet formuleras som ett icke-linjärt minstakvadratproblem, som sedan löses med hjälp av en lokal optimerare kombinerat med en systematisk återstartningsteknik. På så sätt kan flera lösningar presenteras och den lämpligaste kan sedan utses. Programmet har sedan använts till att analysera syntetiska och uppmätta data.		
<b>Nyckelord</b> miljökaraktärisering, återstarter, inversion		
<b>Övriga bibliografiska uppgifter</b>	<b>Språk</b> Engelska	
<b>ISSN</b> 1650-1942	<b>Antal sidor:</b> 55 s.	
<b>Distribution enligt missiv</b>	<b>Pris:</b> Enligt prislista	



# Abstract

This report presents a multistart technique version of an inverse electromagnetic propagation computer program. The program is specialized in calculating the conductivity profile, e.g. the conductivity and the layer depths in a horizontally stratified environment. The problem is formulated as a nonlinear least-squares problem, and to obtain a good solution the program uses a quasi-global optimisation technique. A local optimisation method is used, but a multistart technique results in several solutions, and the solution with the lowest cost function may then be chosen. The program has been used to analyse some synthetic and some measured data. From the analysis two important conclusions has been drawn. First, the synthetic data analysis with one winter and one summer case has shown that it probably is enough to measure the conductivity profile in the sediment and bedrock layers once a year, and just change the water conductivity with the seasons. Second, it is worth noting that going from four to five layers doesn't change the cost function much, so more than five layers, or in some cases more than four layers, are not worth the effort to produce. The measurement errors and above all the model error then dominate.

# Contents

<b>1</b>	<b>Introduction</b>	<b>4</b>
<b>2</b>	<b>The Model</b>	<b>6</b>
2.1	Geometry . . . . .	6
2.2	The Electric and Magnetic Fields . . . . .	7
2.3	The NLayer 2.0 Program . . . . .	7
<b>3</b>	<b>Theory</b>	<b>8</b>
3.1	The INV_NLayer 2.0 Program . . . . .	8
3.1.1	The Levenberg-Marquardt algorithm . . . . .	8
3.1.2	The Cost Function . . . . .	9
3.2	The Vertical E-field Component . . . . .	10
<b>4</b>	<b>The INV_NLayer_RESTART Program</b>	<b>11</b>
<b>5</b>	<b>Three and Four Layer Solutions : Synthetic data</b>	<b>13</b>
5.1	Summer and Winter Definitions . . . . .	13
5.2	Three Layers . . . . .	14
5.2.1	Winter Profile . . . . .	15
5.2.2	Summer Profile . . . . .	21
5.3	Four Layers . . . . .	26
5.3.1	Winter Profile . . . . .	26
5.3.2	Summer Profile . . . . .	28
5.4	Summer and Winter Results . . . . .	29
<b>6</b>	<b>Three and Four Layer Solutions : Measured data</b>	<b>32</b>
6.1	The Trial . . . . .	32
6.2	Sequence Transmissions . . . . .	33
6.2.1	Three Layers . . . . .	33
6.2.2	Four Layers . . . . .	37
6.3	Square Wave Transmission . . . . .	41
6.3.1	Three Layers . . . . .	41
6.3.2	Four Layers . . . . .	43

<b>7</b>	<b>Algorithm for five layers</b>	<b>45</b>
7.1	Winter Results . . . . .	46
7.2	Measured Data Results . . . . .	47
7.2.1	Sequence Transmissions . . . . .	47
7.2.2	Square Wave Transmissions . . . . .	48
<b>8</b>	<b>Conclusions</b>	<b>50</b>



# Chapter 1

## Introduction

A common problem for the marine defence is the problem of localising submarines, ships and other objects in the water. There are a number of systems designed for this type of problems, and they are based on hydroacoustic or electromagnetic phenomena. The systems can be either passive or active. The passive systems include sensors which detect the sound of or small electromagnetic signature of the vessel. An active system radiates electromagnetic or acoustic energy and the sensors detects the reflected energy and analyses the information.

To analyse the received signal in the sensors whether you have a passive or active system, a good model of the environment is required. In this thesis, a one-dimensional horizontally stratified model is used. The aim is to find effective ways to find important environment parameters such as conductivities and layer depths. In chapter two, this model is more closely presented. The model is also used in the electromagnetic wave propagation computer programs N\_LAYER [1] and INV\_N\_LAYER [7]. These programs will be used to find the best model of the environment, and they are described in chapter three. In this chapter, our problem is also more carefully formulated and some background theory is discussed.

A controlled source can be used to collect data and with the INV\_N\_LAYER program calculate the environment, e.g. the conductivity profile, in the water, sediment bottom and the bedrock. The program formulates the problem as a local least square problem, which sometimes makes it hard to know if the calculated solution is the best solution. This master of science (MSc) thesis will look at ways to improve the INV\_N\_LAYER program. Three different multistart techniques will be implemented to achieve a quasi-global optimisation method. The changes and the addendums in the programs can be closer studied in chapter four. The method will then be used on synthetic data, one wintercase and one summercase. Eventually some measured data will be analysed. This will be implemented in chapter five and six. An algorithm to find a five-layer

model assuming we have an acceptable four-layer model is finally presented in chapter seven.

## Chapter 2

# The Model

### 2.1 Geometry

The first problem when you want to solve problems like this is to find a simple but effective model of the environment. In this case we use a one-dimensional horizontally stratified model. In the example below a five-layer model is presented. Each layer has a constant conductivity and a constant permittivity and they are assumed to be non-magnetic.

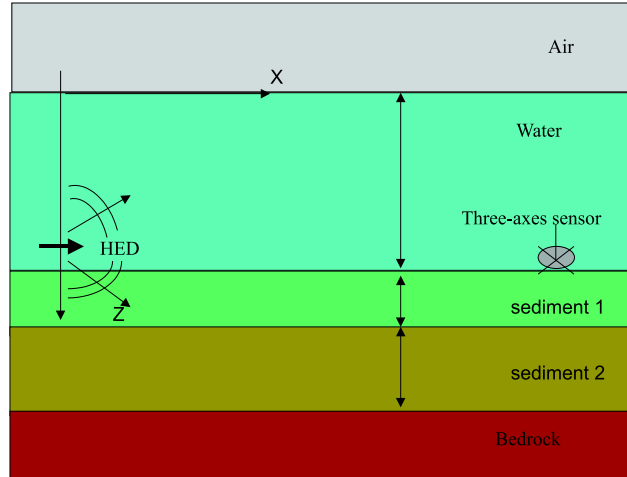


Figure 2.1: A five-layer model

The thickness of the top and the bottom layers are assumed to be infinite. The source and the receiver are placed in the second layer, which symbolises the water. In this thesis, the aim is to find the conductivity profile, e.g. the conductivity in each layer, and the layer depths. The conductivity in the top layer, the air, is assumed to be zero. In the `INV_NLAYER_RESTART` program the conductivity is also assumed to

decrease in each layer, so the sediments cannot have a larger conductivity than the water. This is a reasonable limitation almost everywhere. The source is a horizontal electric dipole (HED), and the receiver is a three-axes sensor. The relative permittivity is assumed to be  $\varepsilon_r = 1$  in the first layer and  $\varepsilon_r = 4$  in the last layer. In the middle layers it is set to  $\varepsilon_r = 81$ . Problems with this type of structure are closely described in [6].

## 2.2 The Electric and Magnetic Fields

There are four fundamental vector field quantities in electromagnetics, the electric field intensity  $\mathbf{E}$ , the electric flux density  $\mathbf{D}$ , the magnetic flux density  $\mathbf{B}$  and the magnetic field intensity  $\mathbf{H}$ . In this thesis only the  $\mathbf{E}$  and the  $\mathbf{B}$  fields are used. The electric field  $\mathbf{E}$  is measured in volts per meter (V/m) and the magnetic field  $\mathbf{B}$  is measured in the SI-unit Tesla (T). A very thorough description of the electromagnetic foundations can be found in [2].

## 2.3 The NLAYER 2.0 Program

The numerical solution to the forward problem is obtained from the program NLAYER 2.0. This program computes ELFE (Extremely Low Frequency Electromagnetics) fields from monofrequent dipole sources in cylindrical geometries with a number of horizontal homogeneous layers. The source and the receiver may be placed in any layer. NLAYER assumes that all layers is nonmagnetic,  $\mu = 4\pi 10^{-7}$  H/m, and that the time-dependence is of the form  $e^{-i\omega t}$ . The fields from the dipole sources are expressed by the Hertz vector  $\Pi$ . The Hertz vector is closer described in [5].

$$\mathbf{H} = (\sigma - i\omega\varepsilon)\nabla \times \Pi \quad (2.1)$$

$$\mathbf{E} = \nabla(\nabla \cdot \Pi) + k^2\Pi \quad (2.2)$$

$$k^2 = i\omega\mu(\sigma - i\omega\varepsilon) \quad (2.3)$$

Since all the layers are non-magnetic,  $\mathbf{B}$  can be expressed as  $\mu_0\mathbf{H}$  and eq. (2.1) can be written as

$$\mathbf{B} = \mu_0(\sigma - i\omega\varepsilon)\nabla \times \Pi \quad (2.4)$$

The solution for the Hertz potential is obtained by Fourier transform techniques and adaptive wave number integrations. More details can be found in [1].

## Chapter 3

# Theory

### 3.1 The INV\_NLAYER 2.0 Program

The INV\_NLAYER computer program is based on the model described in chapter two. Through collection of data from a known source this program can calculate the conductivity profile, the layer depths and other relevant parameters. This is performed by fitting computed electromagnetic data from a model to the experimental data. The parameters are adjusted until the difference between the computed and measured data is small. This is called optimisation, and the INV\_NLAYER program formulates the optimisation problem as a non-linear least squares problem. The sums of the squares of the difference between computed and measured values are then minimised with a suitable algorithm. The optimisation method in the INV\_NLAYER program is a local technique, which means that the computed minima may not be the global minima, i.e. it may not be the best solution. A global technique, such as the genetic algorithm, usually finds the global minima but these methods are slow. Local methods converge more rapidly but depend strongly on the starting vector. This is the largest limitation in the INV\_NLAYER program.

The optimisation algorithms used in INV\_NLAYER are described in the following subsection. The user may choose between the Levenberg-Marquardt algorithm [3], [7] and the regularised Newton-Kantorovich method [3], [9]. In this thesis, all calculations have been done with the Levenberg-Marquardt algorithm.

#### 3.1.1 The Levenberg-Marquardt algorithm

The function  $f(\mathbf{x})$  to be minimised can in this case be written as

$$f(\mathbf{x}) = \|\mathbf{r}(\mathbf{x})\|_2^2 \quad (3.1)$$

where

$$\mathbf{r}(\mathbf{x}) = \mathbf{m}(\mathbf{x}, \mathbf{y}) - \mathbf{d} \quad (3.2)$$

$\mathbf{m}(\mathbf{x}, \mathbf{y})$  is the predicted data set for a certain variable parameter vector  $\mathbf{x}$  (the parameters being estimated) and a constant parameter vector  $\mathbf{y}$ , and  $\mathbf{d}$  is the measured data set. The function  $f(\mathbf{x})$  is then expanded in a Taylor series around the point  $\mathbf{x}_c$ :

$$\begin{aligned}\tilde{f}(\mathbf{x}) &= \frac{1}{2} \mathbf{r}(\mathbf{x}_c)^T \mathbf{r}(\mathbf{x}_c) + \mathbf{r}(\mathbf{x}_c)^T \mathbf{J}(\mathbf{x}_c)(\mathbf{x} - \mathbf{x}_c) \\ &+ \frac{1}{2} (\mathbf{x} - \mathbf{x}_c)^T (\mathbf{J}(\mathbf{x}_c)^T \mathbf{J}(\mathbf{x}_c) + \mathbf{S}(\mathbf{x}_c)) (\mathbf{x} - \mathbf{x}_c)\end{aligned}\quad (3.3)$$

$$\mathbf{S}(\mathbf{x}) = \mathbf{r}(\mathbf{x})^T \nabla^2 \mathbf{r}(\mathbf{x}) \quad (3.4)$$

Where  $\mathbf{J}(\mathbf{x}_c)$  is the Jacobian matrix with respect to  $\mathbf{x}$  at the point  $\mathbf{x}_c$ . The matrix  $\mathbf{S}(\mathbf{x})$  is assumed to be small, and can be neglected. This gives us a vector  $\mathbf{x}_+$  which minimises  $\tilde{f}(\mathbf{x})$

$$\mathbf{x}_+ = \mathbf{x}_c - (\mathbf{J}(\mathbf{x}_c)^T \mathbf{J}(\mathbf{x}_c))^{-1} \mathbf{J}(\mathbf{x}_c)^T \mathbf{r}(\mathbf{x}_c) \quad (3.5)$$

This is an explicit solution for  $\mathbf{x}_+$  if the jacobian has full rank. The vector  $\mathbf{x}_*$  that minimises the vector  $f(\mathbf{x})$  is then computed by using (3.5) at each iteration step.

This is a Gauss-Newton minimisation technique. If  $\mathbf{S}(\mathbf{x}_*)$  is small compared with  $\mathbf{J}(\mathbf{x}_*)^T \mathbf{J}(\mathbf{x}_*)$  the method is linearly convergent. The matrix  $\mathbf{J}(\mathbf{x}_c)^T \mathbf{J}(\mathbf{x}_c)$  needs to be non-singular and positive definite to ensure a Gauss-Newton step in a descent direction. This is a problem, since the method fails to converge if the conditions are not fulfilled. One way to avoid this problem is to restrict the steps for  $\mathbf{x}$  according to the trust region approach

$$\frac{\text{minimise}}{x_+ \in R^n} \|\mathbf{r}(\mathbf{x}_c) + \mathbf{J}(\mathbf{x}_c)(\mathbf{x}_+ - \mathbf{x}_c)\|_2^2 \quad (3.6)$$

$$\text{subjected to } \|\mathbf{x}_+ - \mathbf{x}_c\|_2^2 \leq \delta_c \quad (3.7)$$

The solution to (3.6) and (3.7) is

$$\mathbf{x}_+ = \mathbf{x}_c - (\mathbf{J}(\mathbf{x}_c)^T \mathbf{J}(\mathbf{x}_c) + \mu_c \mathbf{I})^{-1} \mathbf{J}(\mathbf{x}_c)^T \mathbf{r}(\mathbf{x}_c) \quad (3.8)$$

$\mu_c = 0$  if  $\delta_c \geq \|(\mathbf{J}(\mathbf{x}_c)^T \mathbf{J}(\mathbf{x}_c))^{-1} \mathbf{J}(\mathbf{x}_c)^T \mathbf{r}(\mathbf{x}_c)\|_2$ . In this case we get the Gauss-Newton method. If  $\mu_c > 0$  we get another method called the Levenberg-Marquardt minimisation method. The Levenberg-Marquardt method is used in the calculations in the following chapters.

### 3.1.2 The Cost Function

The cost function consists of the sums of squares of the difference between the computed and the measured E-field values. The E-field values are given in dB, so the small values contribute almost as much as the larger

values. The smallest cost function means the best solution in the field point where the sensor is placed, but maybe it doesn't necessarily mean that it is the best solution everywhere. This will be further investigated in later chapters.

## 3.2 The Vertical E-field Component

The vertical E-field component (in this case the z-component) is a lot harder to estimate than the horizontal components. The reason is of course the boundary condition for the E-field when changing medium, e.g.

$$\mathbf{E}_1^{tang} = \mathbf{E}_2^{tang} \quad (3.9)$$

the tangential component of the electric field is continuous across an interface. The normal component on the other hand is discontinuous. The z-component is therefore very sensitive to where the layer boundaries are placed. The x and y components, however, are continuous over the boundaries and aren't as dependent on the layer depths. This is a problem when trying to determine an acceptable conductivity profile.

In this thesis the source used to determine the conductivity profile is a horizontal electrical dipole, a HED. And when trying to find vessels in the water, the vessels are almost always modelled as HED's. A HED has a very weak vertical component, so when trying to localise objects in the water the z-component is so small that it usually is not even measured. This way, the z-component is less important than the other components, so the sensitivity doesn't matter. This is only valid if we are searching the water for objects. If we are for example trying to measure the electromagnetic signature of our ship, it is important to remember that the z-component is as important as the other components.

## Chapter 4

# The INV\_NLAYER\_RESTART Program

The INV\_NLAYER\_RESTART program is one concrete result of this thesis. This program is a modified version of INV\_NLAYER 2.0 and it is designed for calculating the conductivity profile, e.g. optimise on the layer conductivities and depths. The largest difference between the two programs is that the INV\_NLAYER\_RESTART program uses a multistart technique, and the starting vector will be modified between each restart. This way the starting vector isn't as important as in the INV\_NLAYER program. The user may choose between three various techniques to modify the starting vector.

**Random restart** , e.g. each parameter to be estimated is given a random new starting value in a certain interval.

**Systematic stepping** , e.g. the parameter space is divided into a suitable number of equidistant points and one point is used as a starting vector in each restart.

**Random stepping** , e.g. all old values are considered, and a random number is created in the longest interval without any old values. The new value  $\Psi_n$  is chosen randomly in the interval where the difference  $|\Psi_i - \Psi_{i-1}|$  is greatest.  $i$  goes from 1 to  $n$ , and  $\Psi_1$  is the lowest starting value and  $\Psi_{n-1}$  is the greatest value. This method is used in all results presented in later chapters. The technique can be more closely studied in [4].

The INV\_NLAYER\_RESTART program also contains an algorithm to automatically find a five-layer model out of a four-layer model. This algorithm is discussed in chapter seven. To get physical solutions, some



limitations are needed. As mentioned in chapter two, the conductivity is assumed to decrease in each layer. If only two parameters are estimated, the program also plots the cost function. This way it is easier to pinpoint where the deepest minima is located.

## Chapter 5

# Three and Four Layer Solutions : Synthetic data

### 5.1 Summer and Winter Definitions

One problem with the conductivity profile in a marine environment is that it varies with the seasons. In the winter, the water conductivity is approximately constant in the entire layer. But in the summer, the conductivity in the water varies with the depth, e.g. the water needs to be divided into several layers. In this chapter we will investigate two synthetic models, one with summerprofile and one with winterprofile. The aim is to find out wheather all the depths and conductivities need to be estimated several times a year to give a good approximation, or if it is enough to just change the conductivity in the waterlayer. It is also a good test for the INV\_NLAYER\_RESTART program.

Wintermodel		Summermodel	
Air	$\sigma = 0 \text{ S/m}$	Air	$\sigma = 0 \text{ S/m}$
water	$\sigma = 0.8 \text{ S/m}$	water	$\sigma = 0.92 \text{ S/m}$
			$\sigma = 0.8 \text{ S/m}$
			$\sigma = 0.75 \text{ S/m}$
			$\sigma = 0.3 \text{ S/m}$
	$\sigma = 0.3 \text{ S/m}$		$\sigma = 0.3 \text{ S/m}$
	$\sigma = 0.05 \text{ S/m}$		$\sigma = 0.05 \text{ S/m}$
	$\sigma = 0.001 \text{ S/m}$		$\sigma = 0.001 \text{ S/m}$

Figure 5.1: Synthetic winter and summer model

The data were also contaminated with white noise, with SNR (signal to noise ratio) = 20 dB, but that didn't affect the result much. Therefore, all results presented here are without noise.

## 5.2 Three Layers

To start with, consider a three-layer model produced from the synthetic data presented above. The problem now looks like in fig (5.2), with the unknown parameters marked red.

The conductivity in the water is assumed to be known, since it is relatively easy to measure. The parameter  $\sigma_{water}$  differs in the summer and the winter case though. In the wintercase  $\sigma_{water} = 0.8$ , and in the summercase we have, as illustrated in fig (5.1),  $\sigma_{water} = 0.92$  when  $0.0 \leq d \leq 8.0$ ,  $\sigma_{water} = 0.8$  when  $8.0 \leq d \leq 18.0$ , and  $\sigma_{water} = 0.75$  when  $d \geq 18$ .



Figure 5.2: A three-layer model

Now the INV\_NLAYER\_RESTART program is used with 500 restarts, using the Levenberg-Marquardt optimisation algorithm to find the best three-layer model. To get an idea of how good the approximation is we then look at the relative errors, both in the actual sensor and three control sensors, placed as fig (5.3) illustrates.

The green circle represents the location of the source, a HED. The sensor marked 1 is the sensor used for the collection of data, the sensors marked 2, 3 and 4 are 5, 1000 and 2000 meters away from the source. All sensors are placed close to the actual bottom of the sea (i.e.  $z = 40$  meters).

Another important issue is how much information of the field is needed. Three different cases are investigated in this section. In the first case, we measure the phases and the amplitudes of the E and B fields. This is however hard to do in real life, so we also look at a more realistic case, when we know the amplitudes of the E-field x, y and z components. The last case is a worst-case scenario, when we only know the magnitude of the total E-field.

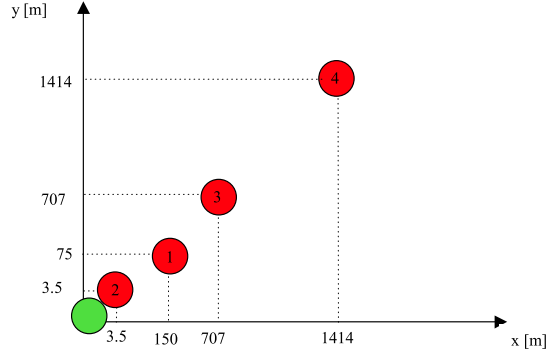


Figure 5.3: The positions of the sensors

### 5.2.1 Winter Profile

By means of the synthetic data created from the winter profile in fig (5.1) the INV\_NLAYER\_RESTART program is used to find a good three-layermodel. The conductivity in the water is easy to measure, so we assume that it is known. Our problem is formulated according to fig (5.2).

#### Phase and Amplitude Information of the E and B Field

Assuming we have information about the E and B fields the INV\_NLAYER\_RESTART program calculates 500 restarts, and one solution turns out to be sufficiently better than the others.

Solution :

depth  $d_1 = 51.54982$

conductivity  $\sigma_1 = 1.63396 \cdot 10^{-3}$  S/m

cost function 0.80552

This result was obtained in 74.8 % of the restarts. All other solutions were either too bad (had too high cost functions) or did not converge.

Now we can look at the relative errors in the four sensors as described in fig (5.3). First, we look only at the horizontal components (the x and y components).

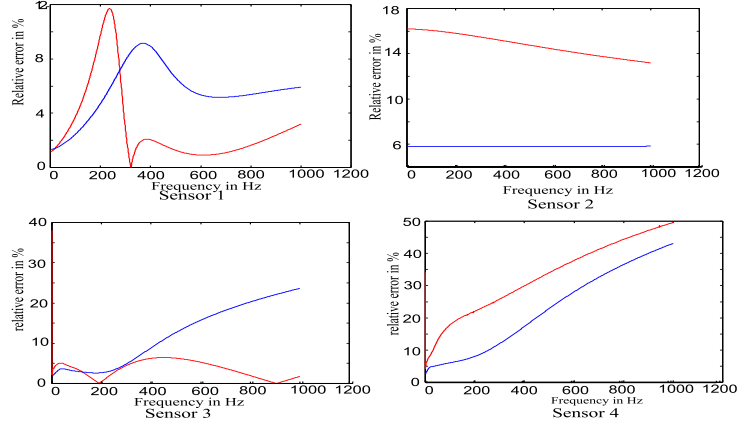


Figure 5.4: Relative error in % for the x(red) and y(blue) components. Winter profile, three layers, phase and amplitude information.

The z-component is a much more delicate problem, and the relative errors in this component are considerably larger. This is illustrated in fig (5.5).

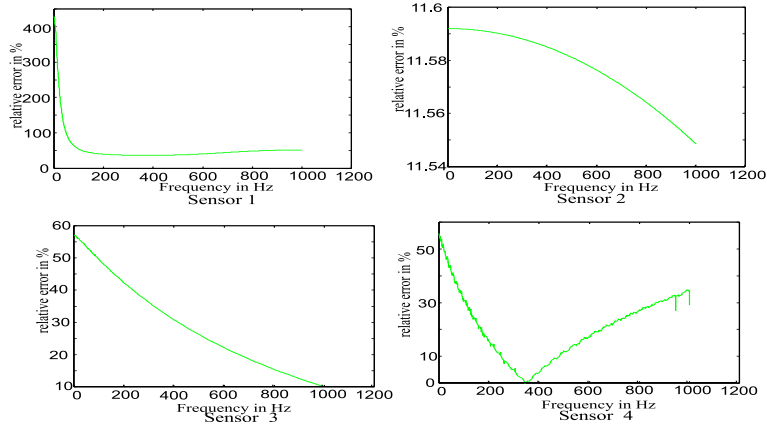


Figure 5.5: Relative error in % for the z component. Winter profile, three layers, phase and amplitude information.

### Information About the Amplitudes of the E-field Components

The more realistic case where we know only the amplitudes of the E-field components gives two possible solutions. The cost function in this case is

illustrated in fig (5.6). The solutions are :

Solution 1 :

depth  $d_1 = 51.54999$

conductivity  $\sigma_1 = 1.02358 \cdot 10^{-3}$  S/m

cost function  $1.09614 \cdot 10^{-2}$

Solution 2 :

depth  $d_1 = 52.46731$

conductivity  $\sigma_1 = 9.74208 \cdot 10^{-4}$  S/m

cost function  $4.76429 \cdot 10^{-2}$

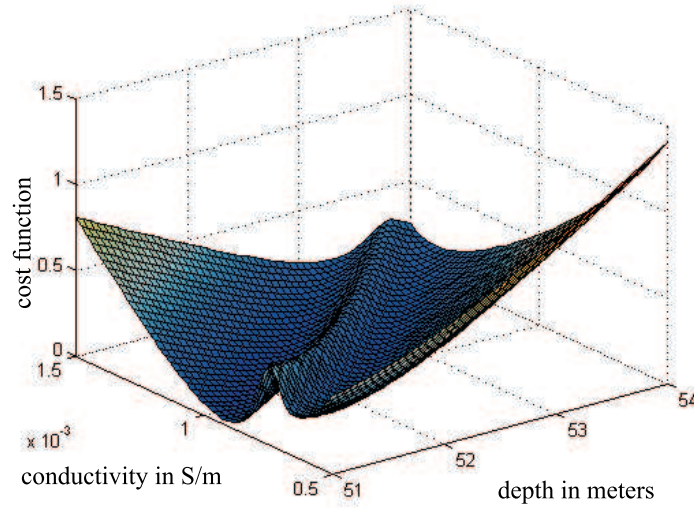


Figure 5.6: The cost function

Solution 1 was obtained in 27.0 % of the restarts, and solution 2 was obtained in 37.0 % of the restarts. The cost functions are so close to each other that it is almost impossible to tell which solution is the best. To get an idea of if one is better than the other the relative errors are studied. The relative errors in the horizontal components are compared in fig (5.7) and the more complicated vertical components are compared in fig (5.8).

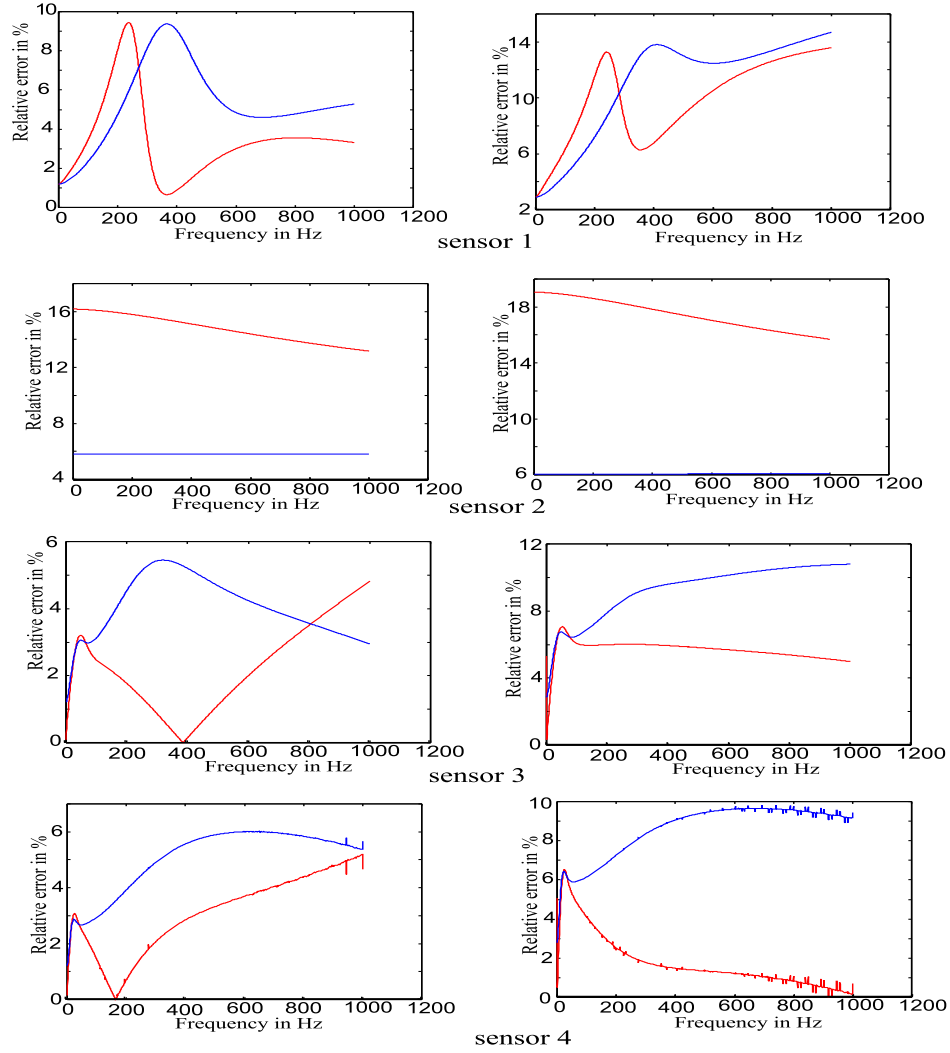


Figure 5.7: Relative errors in the x(red) and y(blue) components. Solution 1 at the left, solution 2 at the right side. Winter profile, three layers, amplitude of the E-field components information.

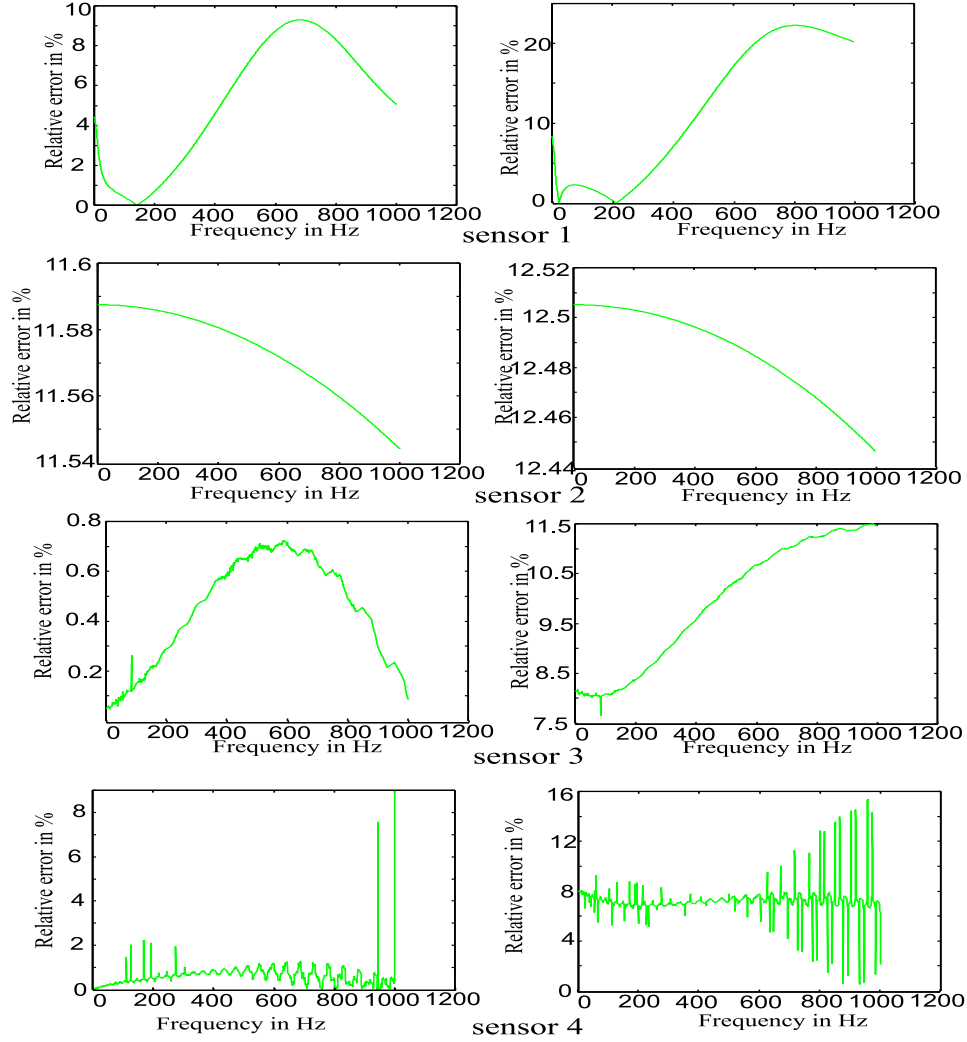


Figure 5.8: Relative errors in the z-components. Solution 1 at the left, solution 2 at the right side. Winter profile, three layers, amplitude of the E-field components information.

We can see that solution 1 is a little better than solution 2. This is expected, since the data are synthetic. For synthetic data the solution with the lowest cost function almost always turns out to be the best.

### Information About the Total E-field Magnitude

The worst case is when we only can measure the magnitude of the total E-field. In this case we get one solution sufficiently better than all other solutions.



Solution :

depth  $d_1 = 50.91756$

conductivity  $\sigma_1 = 7.78285 \cdot 10^{-3}$  S/m

cost function  $7.35191 \cdot 10^{-4}$

This solution was obtained in 64.4 % of the restarts. The relative errors turn out to be larger than in the other cases, as illustrated in fig (5.9) and (5.10).

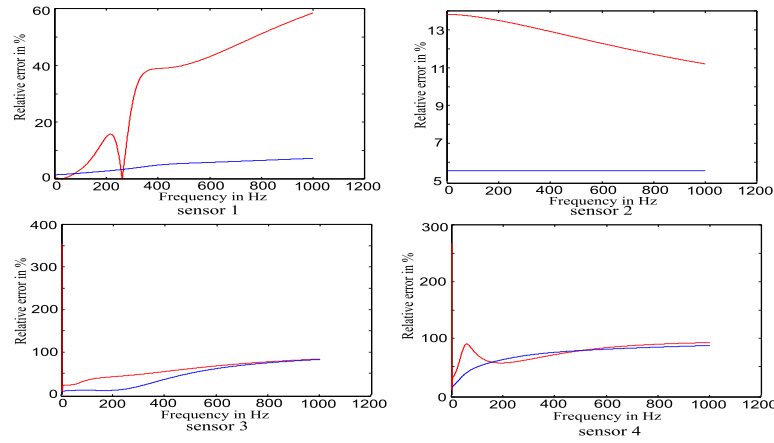


Figure 5.9: Relative errors in the x(red) and y(blue) components. Winter profile, three layers, total E-field magnitude information.

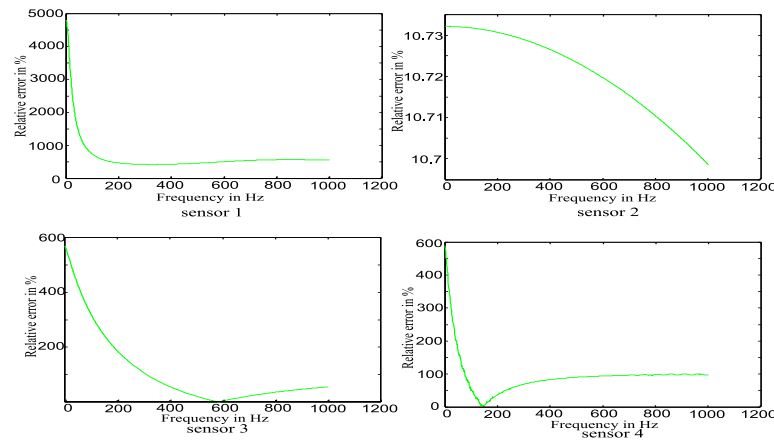


Figure 5.10: Relative errors in the z component. Winter profile, three layers, total E-field magnitude information.

### 5.2.2 Summer Profile

Now the synthetic data are created from the summer profile, and the INV\_NLAYER\_RESTART program calculates the best three-layermodel for this case too. The conductivity is assumed known, and 500 restarts in each case are done, using the Levenberg-Marquardt optimisation technique.

#### Phase and Amplitude Information of the E and B Field

In the first case, only one probable solution was obtained.

Solution :

depth  $d_1 = 51.87037$

conductivity  $\sigma_1 = 1.59142 \cdot 10^{-3}$  S/m

cost function 0.73651

This solution was obtained in 53.4 % of the restarts. Overall, the summercase seems as a harder problem than the wintercase. The statistics show that in the wintercase the program finds the good solutions more often than in the summercase. The relative errors in this case can be studied in fig (5.11) and fig (5.12). Comparing this result with the winter result, one can see that the relative errors are very similar.

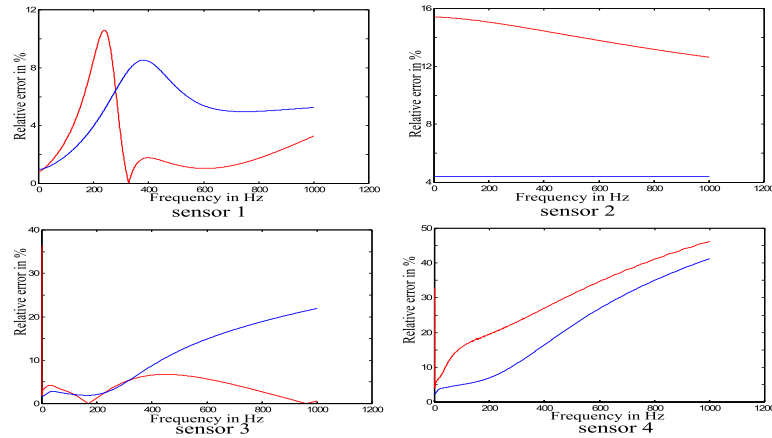


Figure 5.11: Relative errors in the x(red) and y(blue) components. Summer profile, three layers, phase and amplitude information.

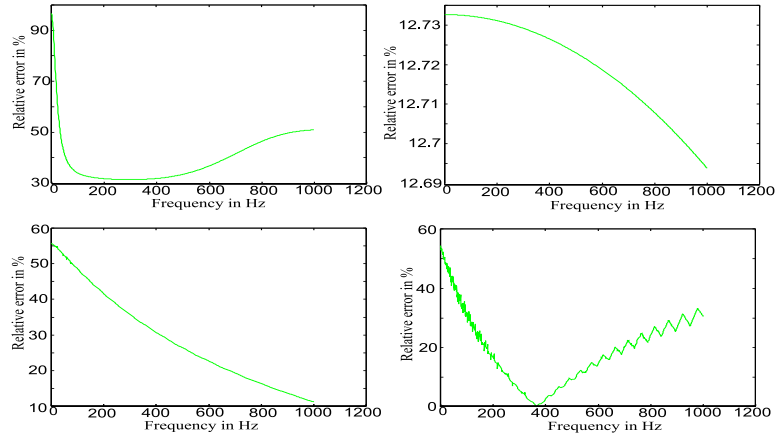


Figure 5.12: Relative errors in the z component. Summer profile, three layers, phase and amplitude information.

### Information About the Amplitudes of the E-field Components

In the summer case, as in the winter case, we get two solutions when information about the E-field components are available. The solutions are close to the winter solutions. The first solution was obtained in 12.0 % of the restarts and the second in 67.2%.

Solution 1:

depth  $d_1 = 50.92999$

conductivity  $\sigma_1 = 1.10908 \cdot 10^{-3}$  S/m

cost function  $5.43189 \cdot 10^{-3}$

Solution 2:

depth  $d_1 = 52.07535$  m

conductivity  $\sigma_1 = 1.03331 \cdot 10^{-3}$  S/m

cost function  $1.20838 \cdot 10^{-2}$

The relative errors can be studied in fig (5.13) and fig (5.14). The errors are in this case too similar to the errors in the winter case. One important thing to notice is that in this case it seems as if solution 2 is the best solution in the sensors, even though solution 1 had the lowest cost function. This tells us that the solution with the best cost function isn't always the best solution !

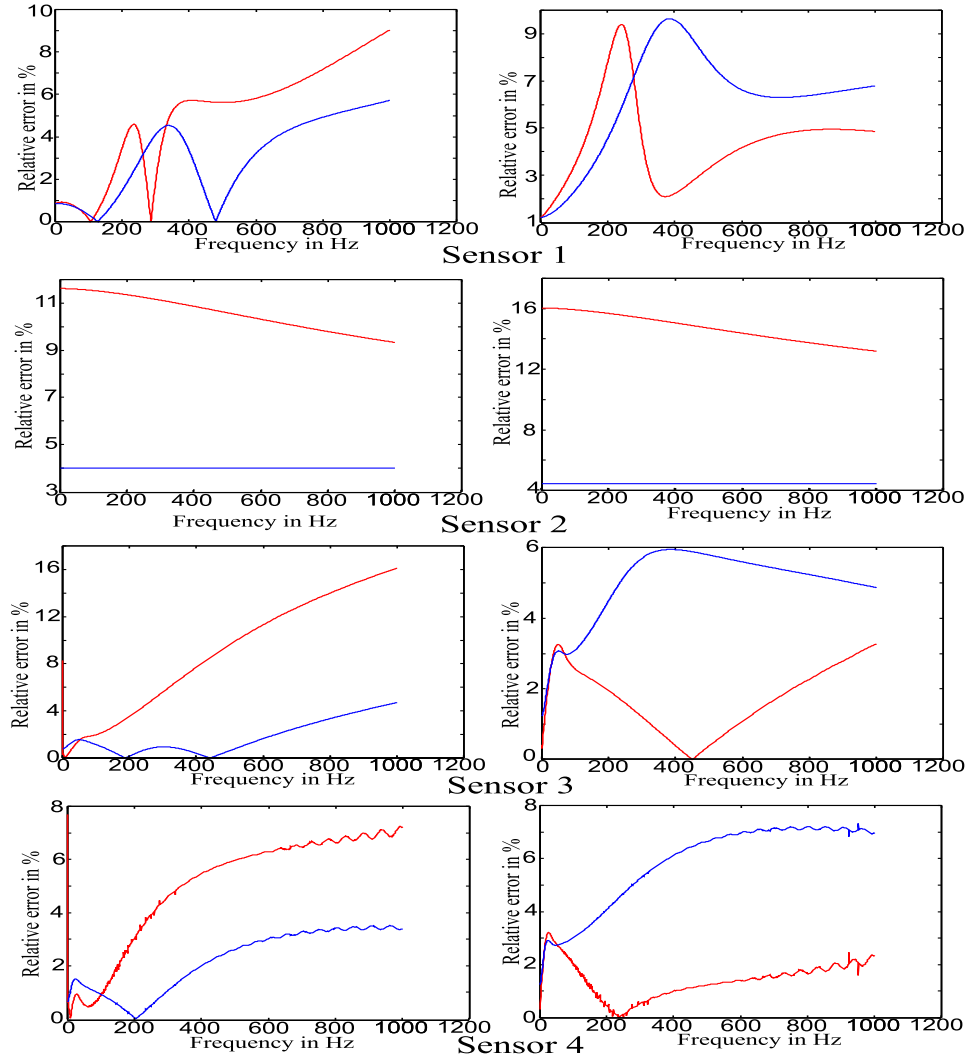


Figure 5.13: Relative errors in the x(red) and y(blue) components. Solution 1 at the left, solution 2 at the right side. Summer profile, three layers, amplitude of the E-field components information.

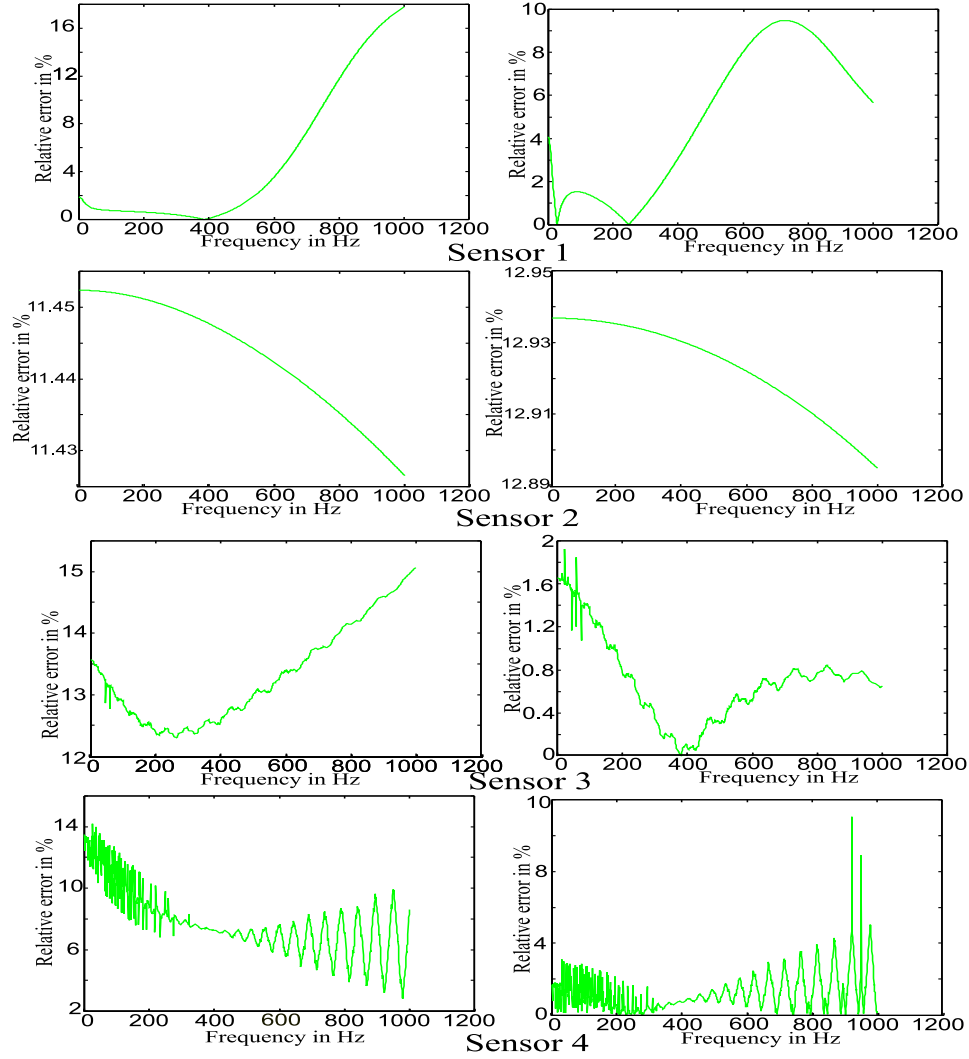


Figure 5.14: Relative errors in the z component. Solution 1 at the left, solution 2 at the right side. Summer profile, three layers, amplitude of the E-field components information.

### Information About the Total E-field Magnitude

One solution was obtained in 15.2 % of the restarts.

Solution :

depth  $d_1 = 51.25919$  m

conductivity  $\sigma_1 = 8.16512 \cdot 10^{-3}$  S/m

cost function  $5.03073 \cdot 10^{-4}$

The relative errors can be studied in fig (5.15) and fig (5.16).

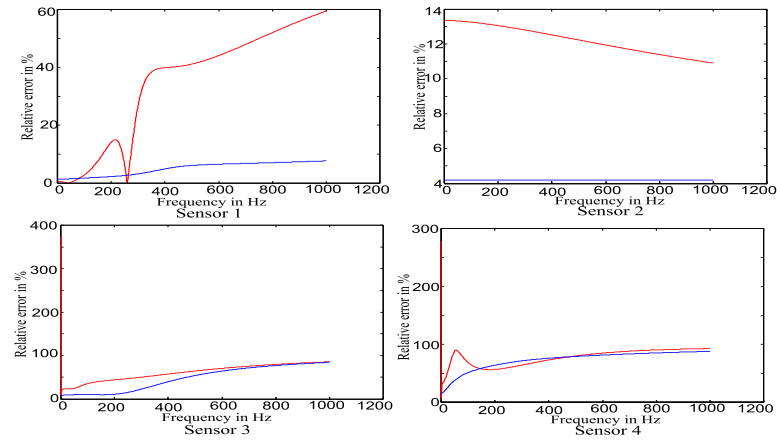


Figure 5.15: Relative errors in the x(red) and y(blue) components. Summer profile, three layers, total E-field magnitude information.

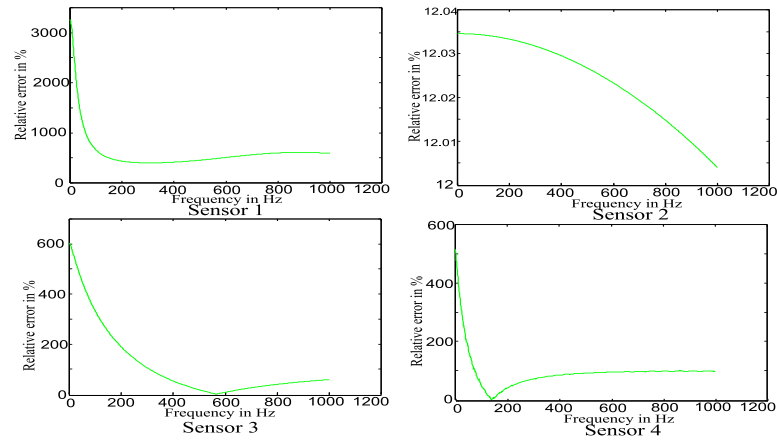


Figure 5.16: Relative errors in the z component. Summer profile, three layers, total E-field magnitude information.

## 5.3 Four Layers

In the four-layer approximation, one depth is assumed to be known. The physical bottom of the sea is easy to measure, and logically one boundary ought to be there. We now have three parameters to estimate, one depth and two conductivities. Our problem is formulated according to fig (5.17) where the parameters to be estimated has been marked red.

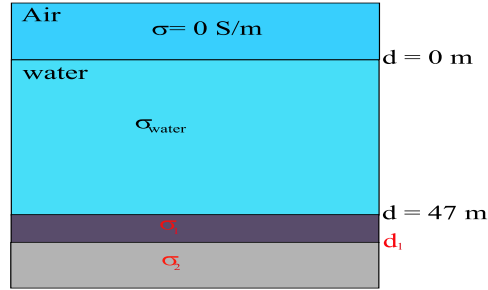


Figure 5.17: A four-layer model.

We now only look at the most common situation, namely the situation when information about the amplitudes of the E-field components is available.

### 5.3.1 Winter Profile

In the winter case, we get one possible solution. We have three parameters to estimate this time instead of two, and that is apparent in the statistics, since fewer restarts converge.

Solution :

depth  $d_1 = 60.87792$

conductivity  $\sigma_1 = 0.22257 \text{ S/m}$

$\sigma_2 = 1.01355 \cdot 10^{-3} \text{ S/m}$

cost function  $3.87403 \cdot 10^{-5}$

This solution was obtained in 16.8 % of the restarts. The relative errors can be studied in fig (5.18) and (5.19).

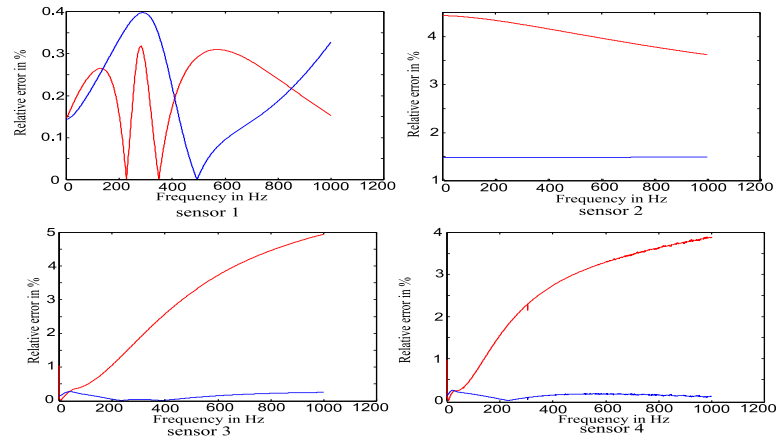


Figure 5.18: Relative errors in the x(red) and y(blue) components. Winter profile, four layers.

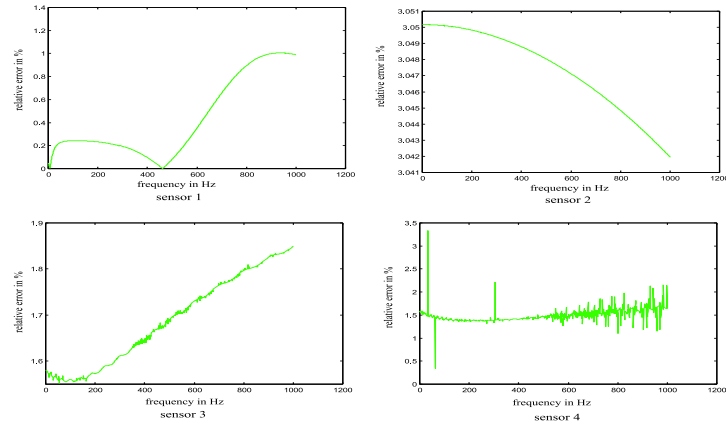


Figure 5.19: Relative errors in the z component. Winter profile, four layers.



### 5.3.2 Summer Profile

In the summer case we also get one probable solution, which is obtained in only 3.0 % of the restarts. It is worth noting that this solution is very similar to the winter solution. How similar will be studied in chapter 5.4.

Solution :

depth  $d_1 = 61.32645$

conductivity  $\sigma_1 = 0.22291$  S/m

$\sigma_2 = 1.00473 \cdot 10^{-3}$  S/m

cost function  $1.43687 \cdot 10^{-4}$

The relative errors, displayed in fig (5.20) and fig (5.21), are also close to the errors in the winter solutions.

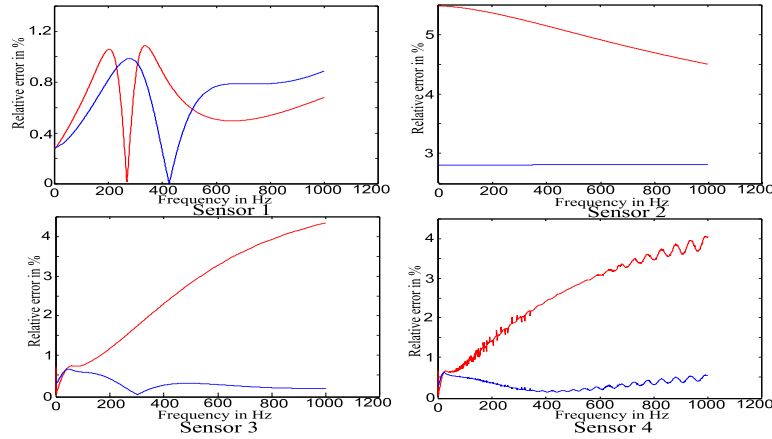


Figure 5.20: Relative errors in the x(red) and y(blue) components. Summer profile, four layers.

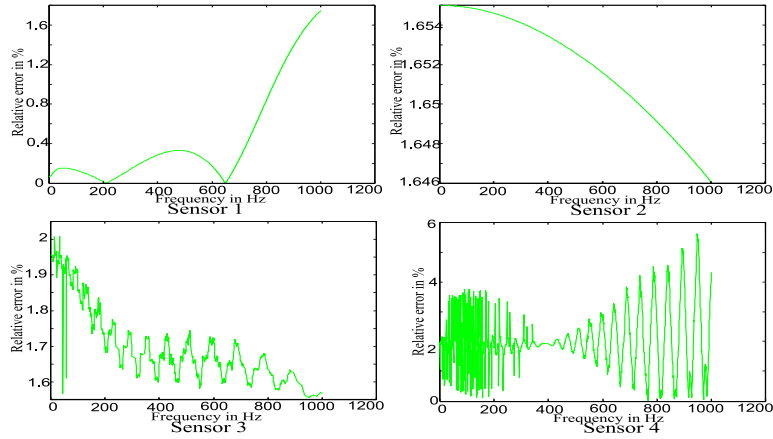


Figure 5.21: Relative errors in the z component. Summer profile, four layers.

## 5.4 Summer and Winter Results

It is important to know if the conductivity profile below the physical sea bottom needs to be altered with the seasons or if it is enough to have one profile the entire year, and just change the conductivity in the water. To get a rough idea of the size of the relative errors in the summer if the profile measured in the winter is used, the solution from the winter calculations is inserted into the summer case. The relative errors in all sensors are then studied.

### Three Layers

For the three-layer model the relative errors are displayed in fig (5.22) (horizontal components) and in fig (5.23) (vertical component). Comparing with the relative errors in the three-layer winter case, fig (5.7) and fig (5.8), one can see no big differences. This indicates that it may be enough to measure the conductivity profile once and use it during all seasons. But before jumping to conclusions the four-layer case should also be investigated.

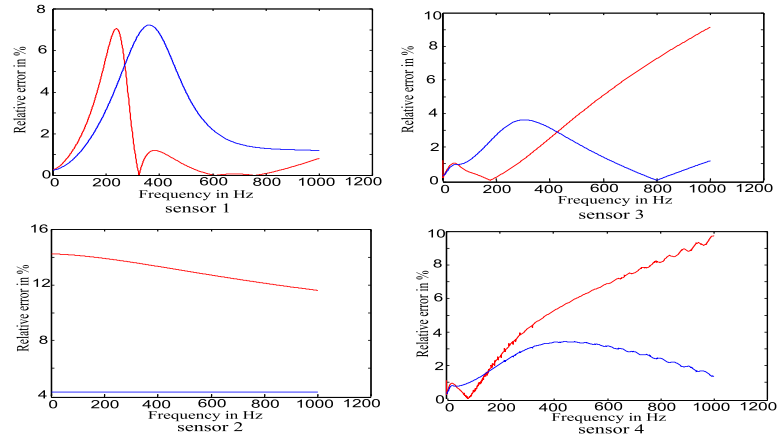


Figure 5.22: Relative errors in the x and y components. Comparison between summer and winter profiles, three layers.

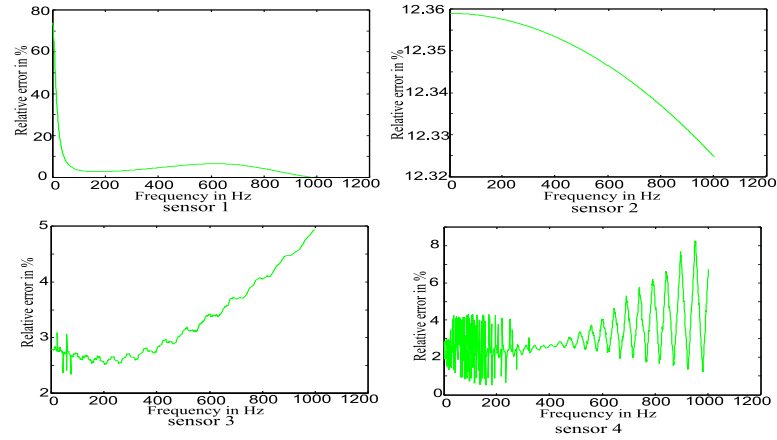


Figure 5.23: Relative errors in the z component. Comparison between summer and winter profiles, three layers.

## Four Layers

For the four-layer model the relative errors are displayed in fig (5.24) and fig (5.25). In this case the relative errors compared with the winter case,

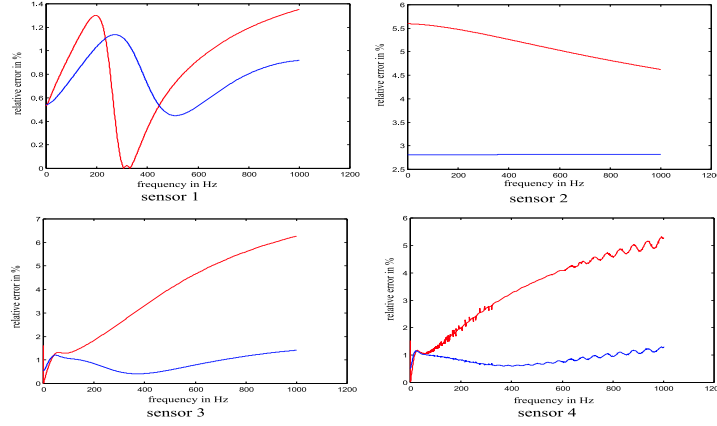


Figure 5.24: Relative errors in the x and y components. Comparison between summer and winter profiles, four layers.

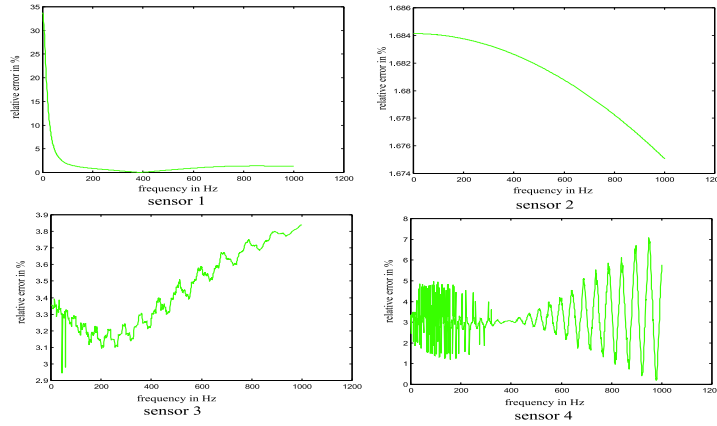


Figure 5.25: Relative errors in the z component. Comparison between summer and winter profiles, four layers.

fig (5.18) and fig (5.19), are evidently larger, but the differences still aren't very big. This indicates that one sediment conductivity profile may be used the entire year, since other errors as model error and measurement errors are considerably larger.

## Chapter 6

# Three and Four Layer Solutions : Measured data

### 6.1 The Trial

In June 2001 a field trial was performed in the south of the archipelago of Stockholm. The trial was carried out according to fig (6.1). The sensor marked 1 is used as a field point when estimating the profiles, and the sensor marked 2 is used to see how good the conductivity profile approximation is in a different point.

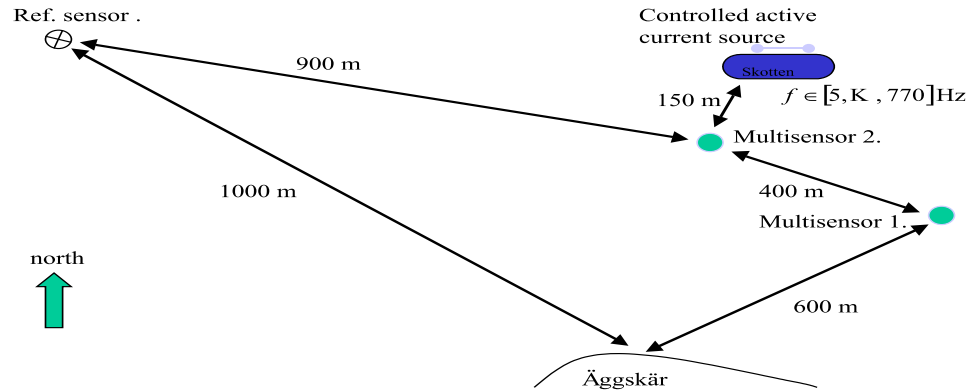


Figure 6.1: The trial.

The physical depth was measured to about 47 meters and the conductivity in the water was about 0.7 S/m. Two various trials were performed. In one case, a sequence of monofrequent transmissions was carried out, and in the other case a square wave was sent out. In the square wave case, the measurement went faster, which means that the sensor didn't have time to move much in the water currents. Because of that, these data are better

than the sequence transmission data.

## 6.2 Sequence Transmissions

### 6.2.1 Three Layers

The data collected in the monofrequent sequence transmission were used to estimate a three-layer model of the environment. After 500 restart two solutions can be presented:

Solution 1 :

depth  $d_1 = 46.79344$

conductivity  $\sigma_1 = 4.17761 \cdot 10^{-2}$  S/m

cost function 0.28614

Solution 2 :

depth  $d_1 = 58.95486$

conductivity  $\sigma_1 = 5.54273 \cdot 10^{-3}$  S/m

cost function 0.89472

We recognize the depth in solution 1 as close to the real physical depth, which was measured to about 47 meters. This solution was obtained in 69.6 % of the restarts, and solution 2 was obtained in 27.0 % of the restarts. To closer investigate the solution the cost function is studied in fig (6.2).

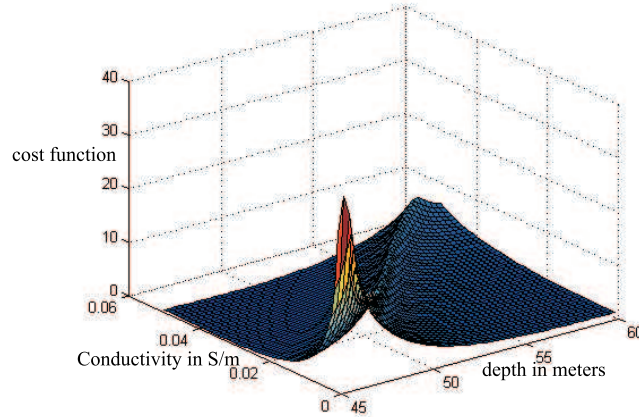


Figure 6.2: The cost function for measured data.

In the figure the two solutions are clearly visible. The E-field components in the field point, sensor 1, are plotted in fig (6.3), where the blue line represents the calculated fields, and the red line is the measured field. The

fields in the reference sensor, sensor 2, are then plotted in fig (6.4). Finally, the relative errors in the both sensors are presented in fig (6.5) and fig (6.6).

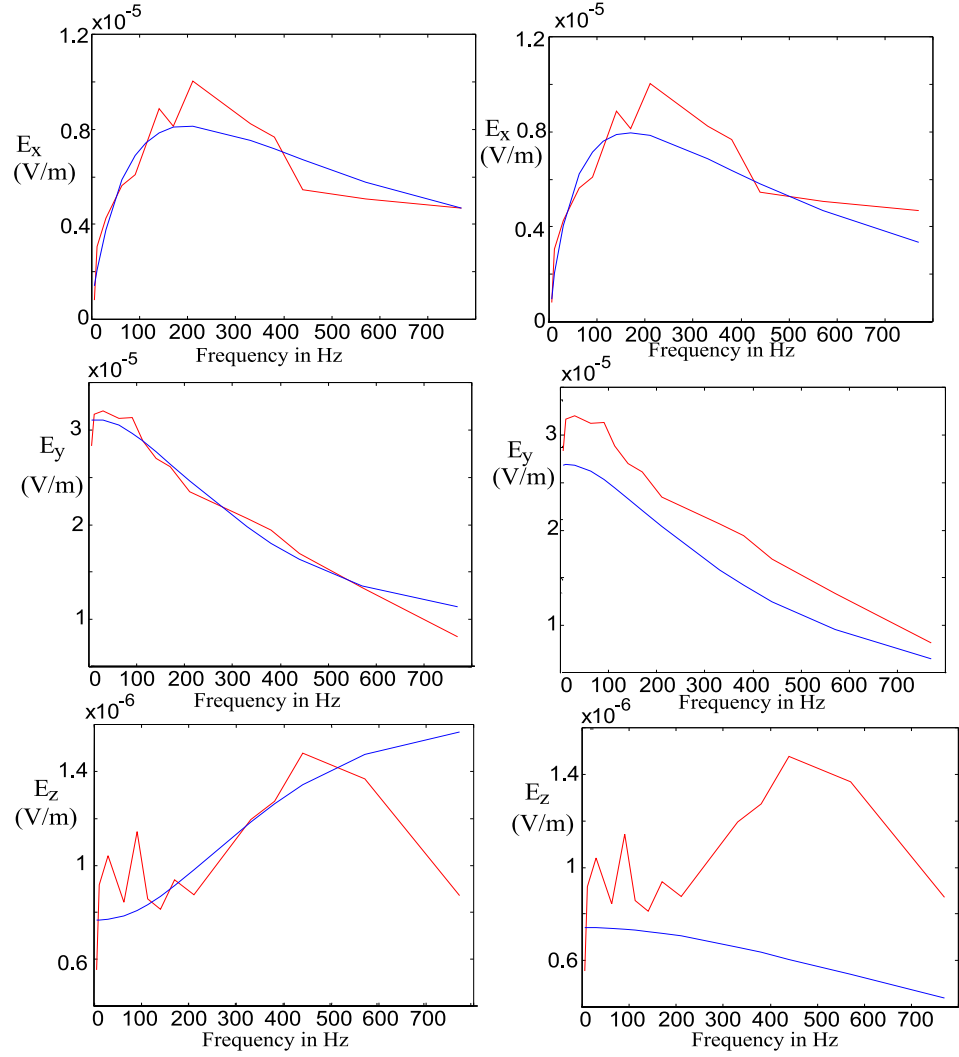


Figure 6.3: The E-field components in sensor 1. Solution 1 at the left side and solution 2 at the right. Sequence transmission, three layers.

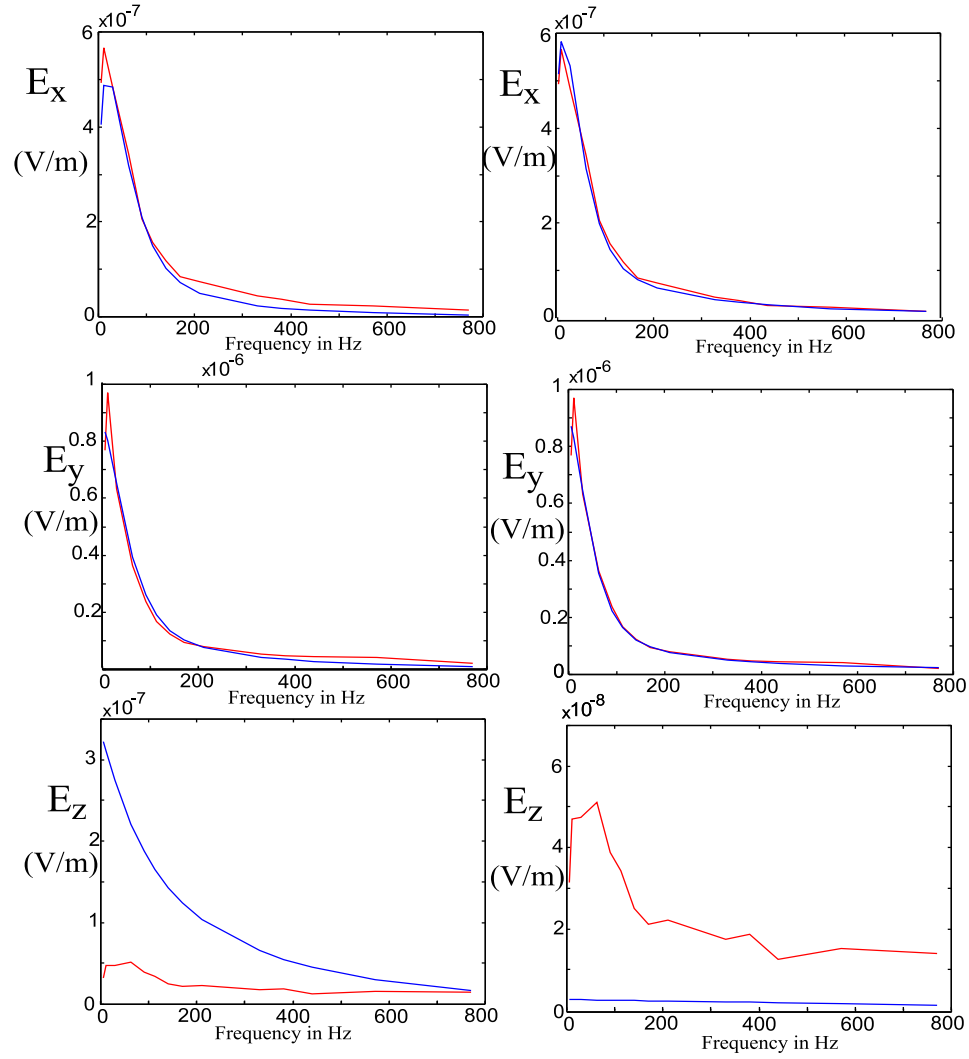


Figure 6.4: The E-field components in sensor 2. Solution 1 at the left side and solution 2 at the right. Sequence transmission, three layers.



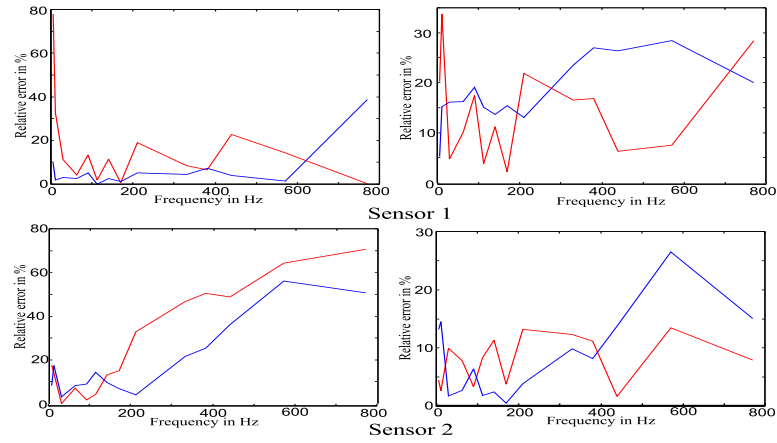


Figure 6.5: The relative errors in the horizontal components. Solution 1 at the left side and solution 2 at the right. Sequence transmission, three layers.

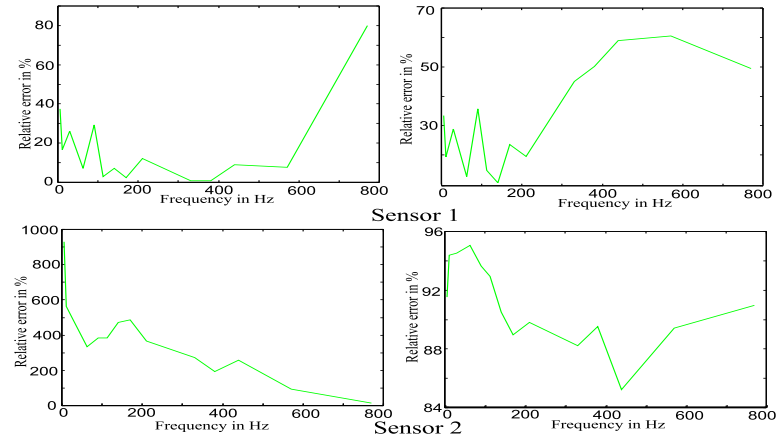


Figure 6.6: The relative errors in the vertical component. Solution 1 at the left side and solution 2 at the right. Sequence transmission, three layers.

### 6.2.2 Four Layers

In the four-layer case the first depth is fixed to 47 meters, and after 500 restarts two solutions are considerably better than all other solutions.

Solution 1 :

depth  $d_1 = 86.04887$  m

conductivity  $\sigma_1 = 0.16172$  S/m

$\sigma_2 = 2.92262 \cdot 10^{-2}$  S/m

cost function 0.27534

Solution 2 :

depth  $d_1 = 51.09906$  m

conductivity  $\sigma_1 = 0.13238$  S/m

$\sigma_2 = 4.22283 \cdot 10^{-2}$  S/m

cost function 0.28467

The first solution was obtained in 52.0 % and the second was obtained in 22.0 % of the restarts. The two solutions can be compared in fig (6.7), (6.8), (6.9) and (6.10).

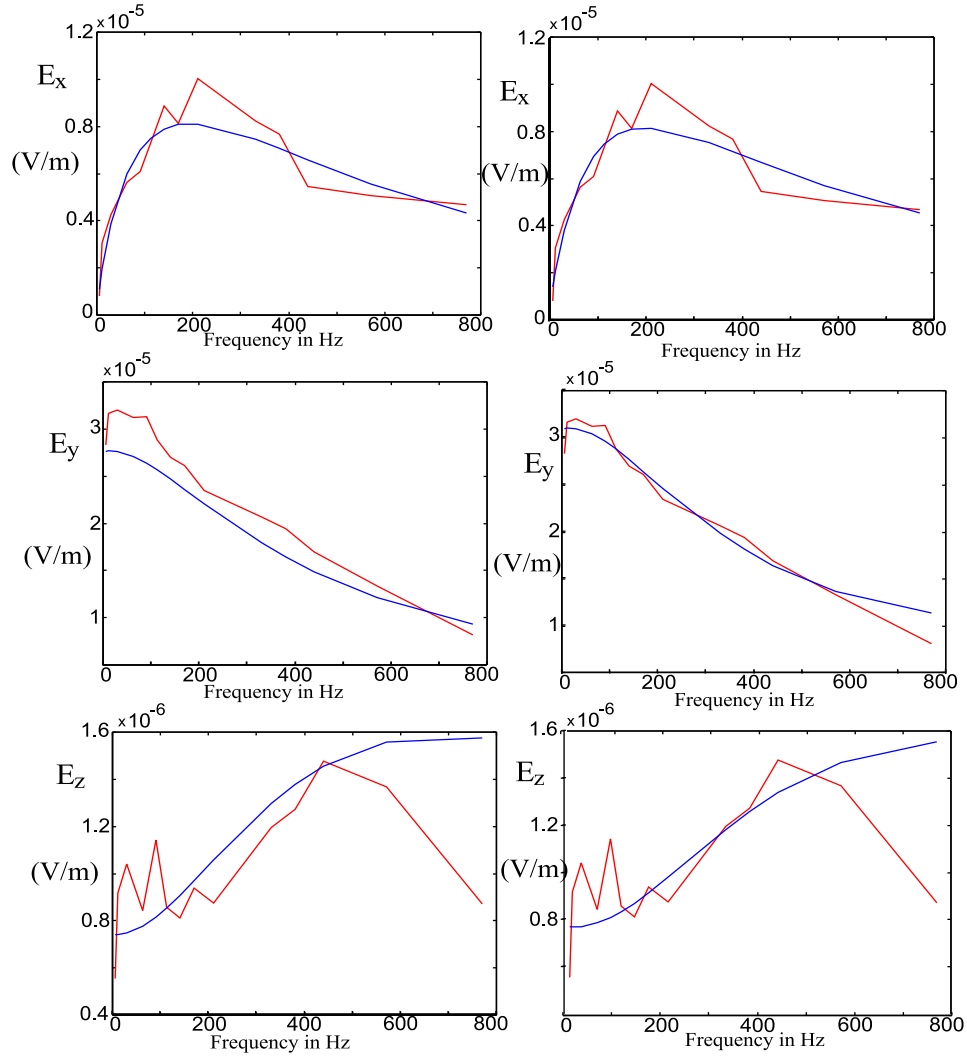


Figure 6.7: The E-field components in sensor 1. Solution 1 at the left side and solution 2 at the right. Sequence transmission, four layers.

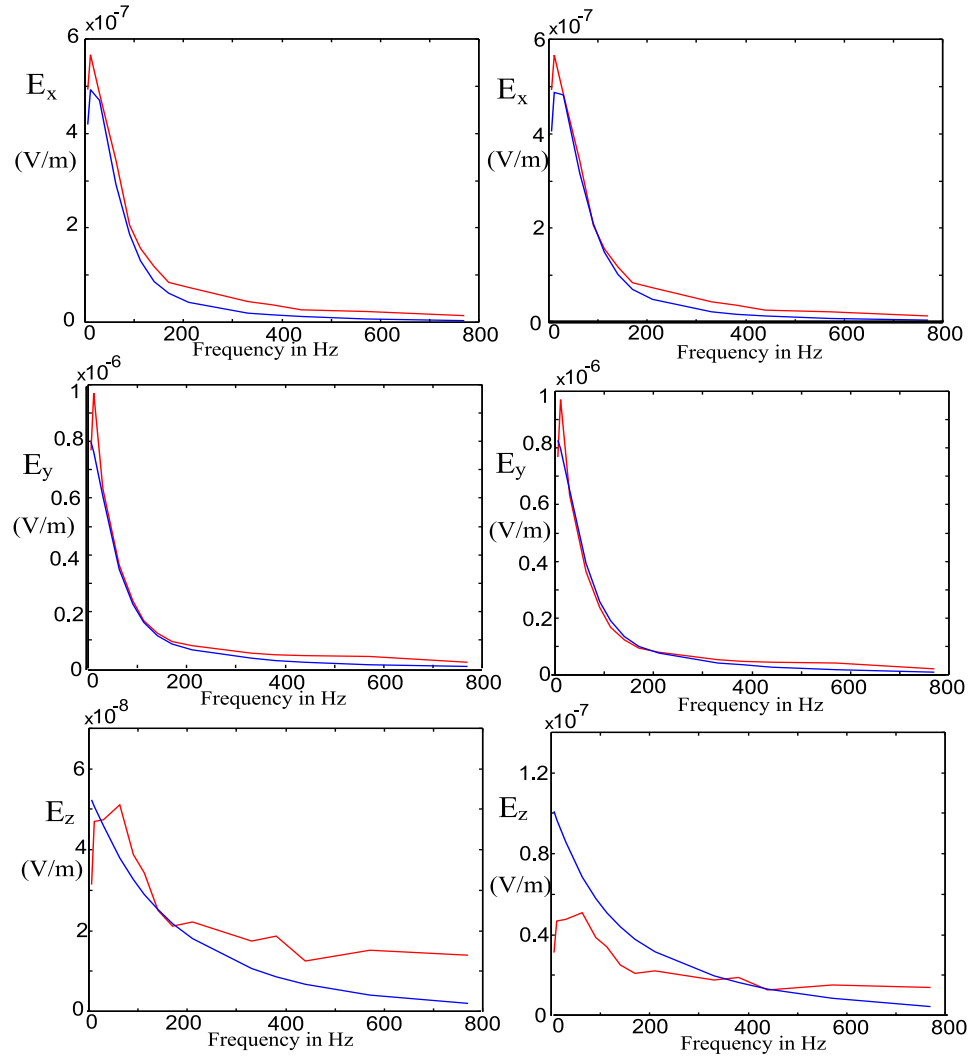


Figure 6.8: The E-field components in sensor 2. Solution 1 at the left side and solution 2 at the right. Sequence transmission, four layers.

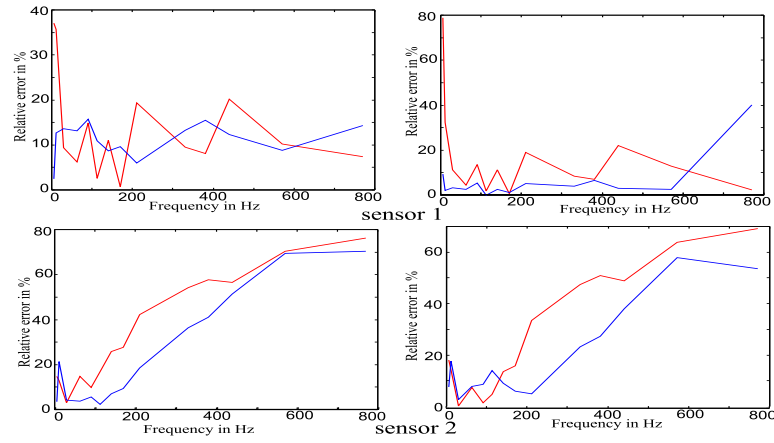


Figure 6.9: The relative errors in the horizontal components. Solution 1 at the left side and solution 2 at the right. Sequence transmission, four layers.

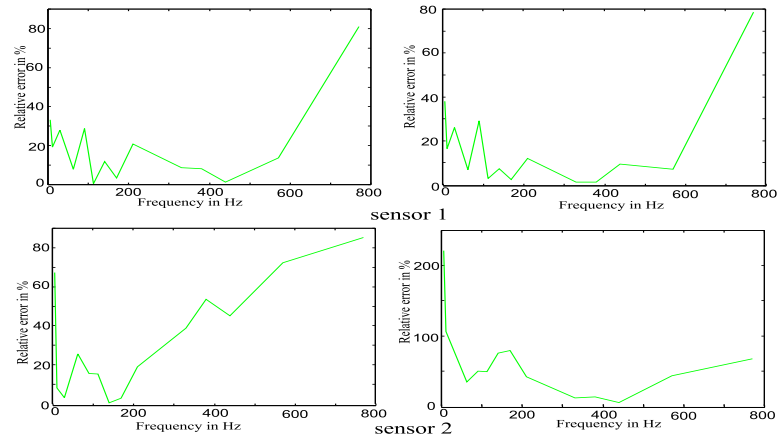


Figure 6.10: The relative errors in the vertical component. Solution 1 at the left side and solution 2 at the right. Sequence transmission, four layers.

## 6.3 Square Wave Transmission

### 6.3.1 Three Layers

When a square wave is transmitted, we run into several problems when trying to estimate good conductivity profiles. In the three-layer case, we find one solution, but it is only obtained in 15.0 % of the restarts.

Solution :

depth  $d_1 = 46.033801$  m

conductivity  $\sigma = 5.46869 \cdot 10^{-2}$  S/m

cost function 0.32724

The electric field in sensor 1 and 2 can be studied in fig (6.12) and the relative errors in fig (6.11).

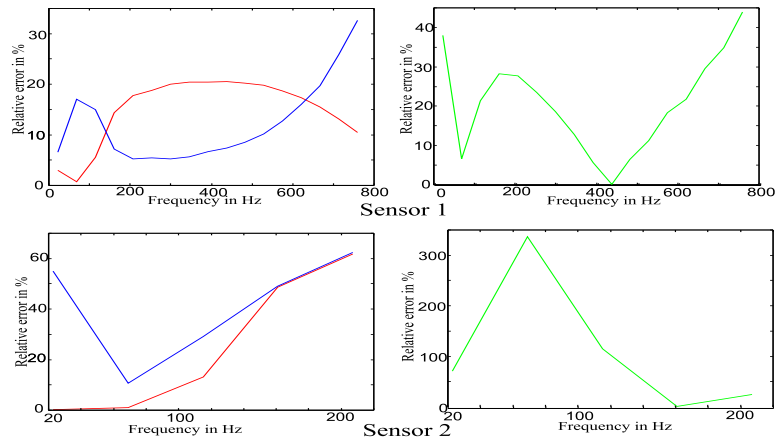


Figure 6.11: The relative errors. Square wave transmission, three layers.

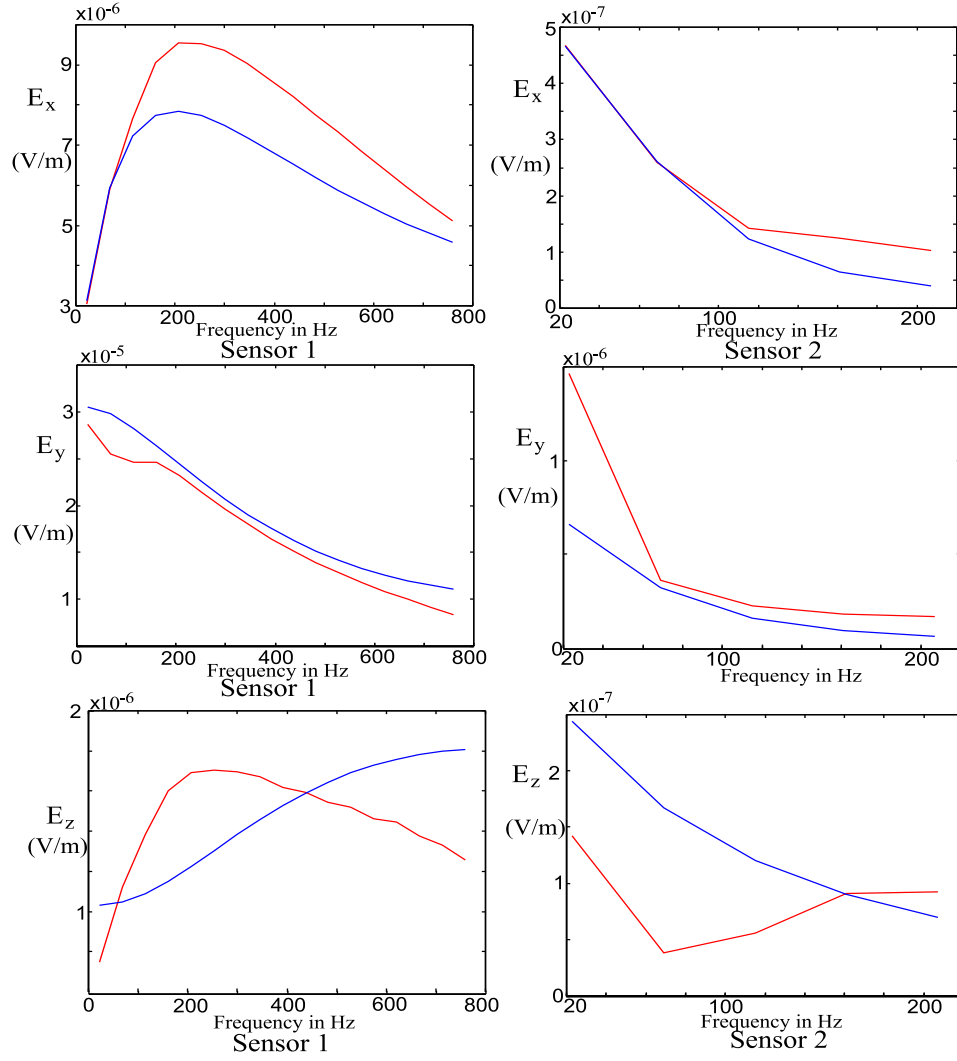


Figure 6.12: Electric fields in sensor 1 and 2. Red line is measured field, blue line is calculated field. Square wave transmission, three layers.

### 6.3.2 Four Layers

In the four-layer case, the bedrock conductivity converges towards zero. This problem cannot be handled by the program, so we have to set the conductivity to a realistic value. In this case it is chosen to  $\sigma_{bedrock} = 0.001$  S/m. One solution is obtained in 66.0 % of the restarts.

Solution :

depth  $d_1 = 107.64657$  m

conductivity  $\sigma_1 = 0.14023$  S/m

$\sigma_2 = 0.001$  S/m (fixed)

cost function 0.22519

The electric field in sensor 1 and 2 can be studied in fig (6.14) and the relative errors in fig (6.13).

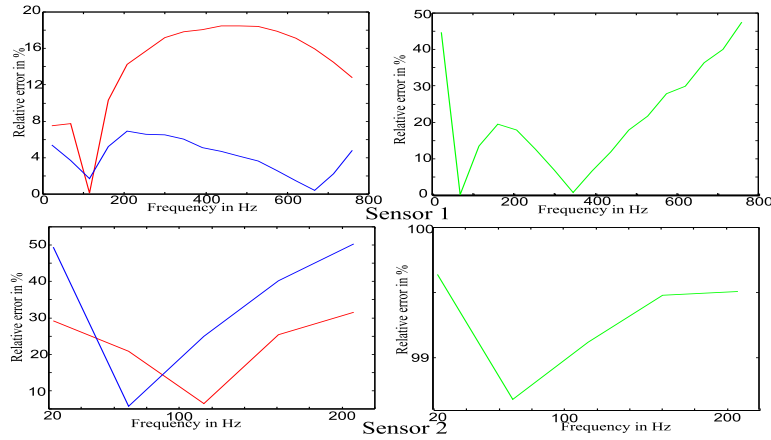


Figure 6.13: The relative errors in the x(red) and y(blue) components at the left side, in the z component at the right. Square wave transmission, four layers.



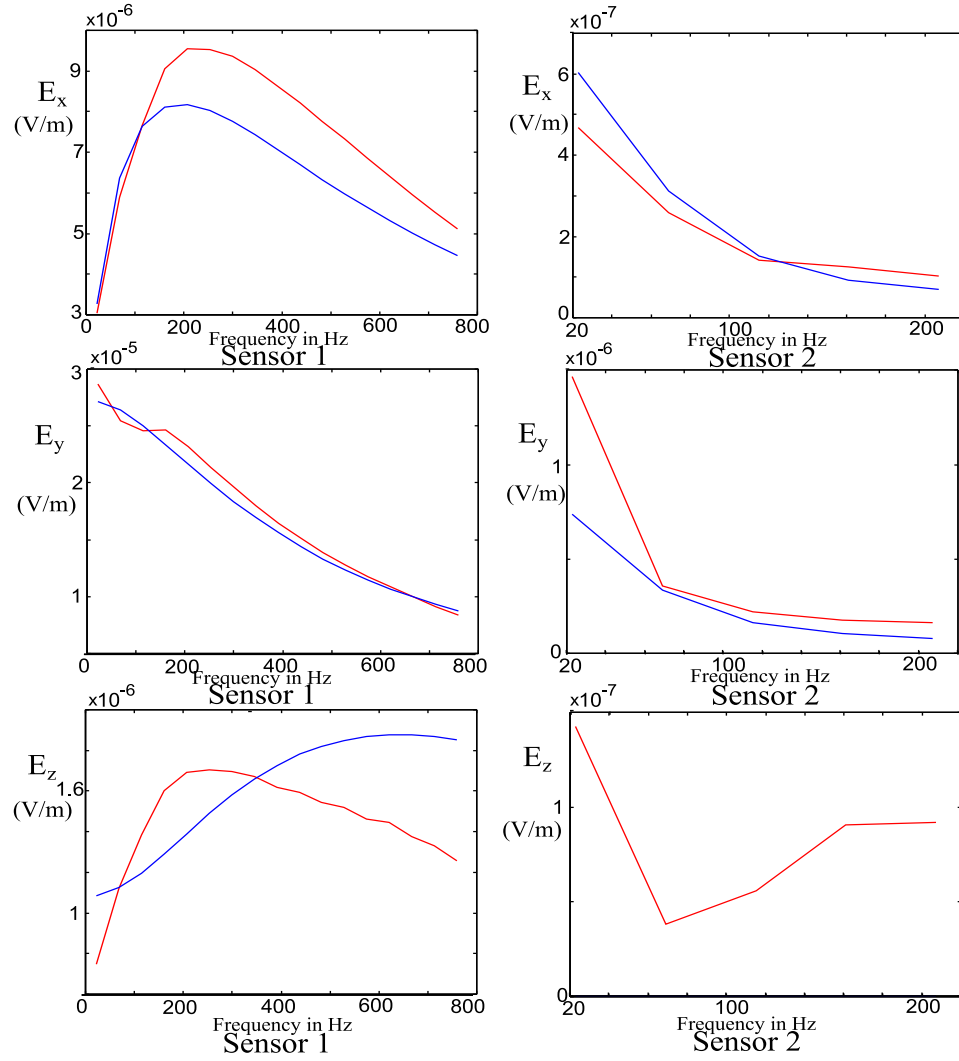


Figure 6.14: Electric field in sensor 1 and 2. Red line is measured field, blue line is calculated field. Square wave transmission, four layers.

## Chapter 7

# Algorithm for five layers

More than four layers are difficult to estimate, since there are many unknown parameters. In this chapter, a four-layer model is calculated, and then another model with more layers are calculated, by means of the four-layer model. This model gives a five-layer model. To get the best four-layer model, the solution with the lowest cost function is chosen by the INV\_NLAYER\_RESTART program. To begin with, a four-layer model is calculated according to fig (5.17). The problem is then how to use this information to calculate a five-layer model. First, one of the parameters estimated needs to be locked. Otherwise, we have too many parameters for the optimisation algorithm to handle. The most realistic scenario is that the conductivity  $\sigma_2$  in fig (5.17) is close to its real value. Therefore, the bottom conductivity is assumed to be known. Our five layer model now looks like fig (7.1), where  $\sigma_{bedrock} = \sigma_2$ . As seen in the figure we have a

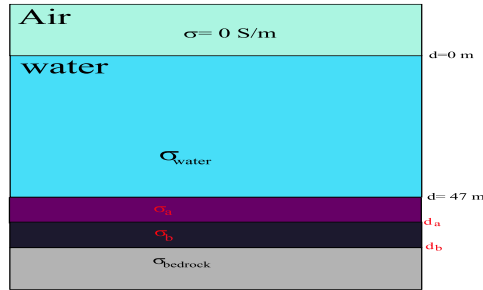


Figure 7.1: A five-layer model.

difficult optimisation problem, since we have four parameters to estimate. To make this work, the parameters must be carefully limited. The two depths  $d_a$  and  $d_b$  are placed as fig (7.2) shows, e.g.  $d_a$  is placed between the known physical sea bottom and the four-layer depth  $d_1$  and the depth  $d_b$  is placed below  $d_1$ . Since the conductivity is assumed to decrease in each

layer, we can also draw the conclusion that  $\sigma_a$  should be in the interval  $\sigma_{water} \leq \sigma_a \leq \sigma_1$  and that  $\sigma_b$  should be in the interval  $\sigma_1 \leq \sigma_b \leq \sigma_{bedrock}$ .

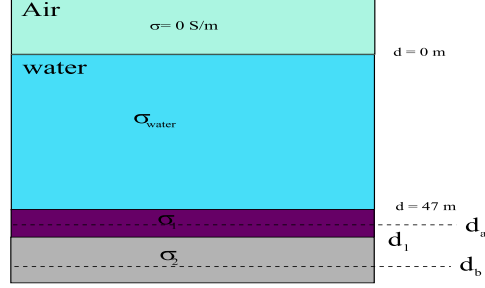


Figure 7.2: The placement of the depths.

With these conditions, a five-layer model can be calculated by the INV\_NLAYER\_RESTART program. The number of restarts are three times greater in the five-layer case compared to the four-layer case. In this case 300 restarts are used in the four-layer case, and 900 in the five-layer case.

## 7.1 Winter Results

The five-layer algorithm is used on the synthetic winter data, and one result is sufficiently better than the other solutions :

Solution :

depth  $d_a = 49.15481 \text{ m}$

$d_b = 63.29086 \text{ m}$

conductivity  $\sigma_a = 0.43383 \text{ S/m}$

$\sigma_b = 0.15544 \text{ S/m}$

$\sigma_{bedrock} = 1.01355 \cdot 10^{-3}$

cost function  $1.30131 \cdot 10^{-5}$

This solution was obtained in 22.0 % of the restarts. The cost function is considerably less than in the four-layer model, and the relative errors in the four sensors can be studied in fig (7.3) and fig (7.4).

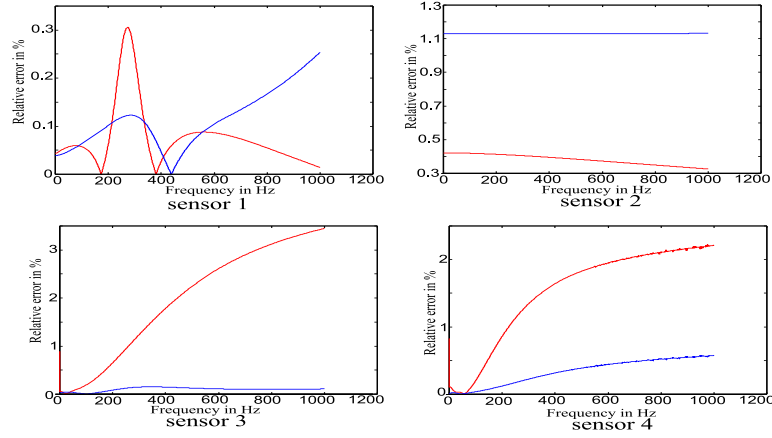


Figure 7.3: Relative errors in the x(red) and y(blue) components. Winter profile, five layers.

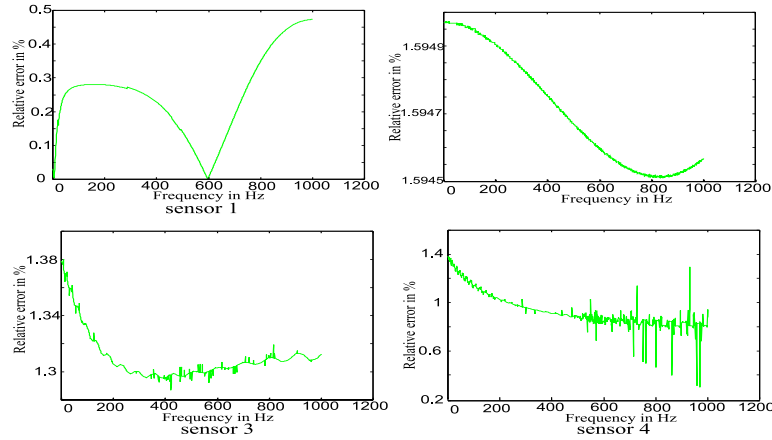


Figure 7.4: Relative errors in the z component. Winter profile, five layers.

## 7.2 Measured Data Results

### 7.2.1 Sequence Transmissions

In the measured data case, the following solution is obtained in 86.0 % of the restarts:

Solution :

depth  $d_a = 65.83371$  m

$d_b = 98.58693$  m

conductivity  $\sigma_a = 0.16661$  S/m  
 $\sigma_b = 9.50423 \cdot 10^{-2}$  S/m  
 $\sigma_{bedrock} = 2.92262 \cdot 10^{-2}$  S/m  
cost function 0.27037

The cost function has not improved as much as one may expect. The relative errors displayed in fig (7.5) are almost the same as in the four layer case. This tells us that it is not worth the effort to use more layers, since the model isn't exact enough. This is about as good as it gets.

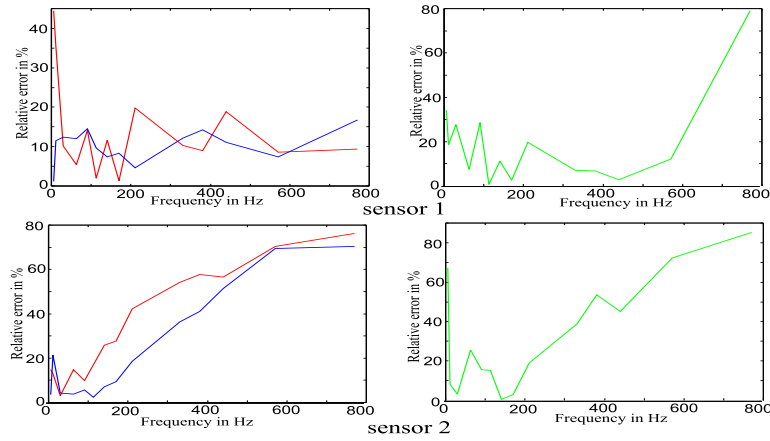


Figure 7.5: Relative errors in the x(red) and y(blue) component at the left and in the z component at the right side. Sequence transmission, five layers.

## 7.2.2 Square Wave Transmissions

The square wave data has turned out to be a very tricky problem for the INV\_NLAYER\_RESTART program. Only in 2.0 % of the restarts a solution was found.

Solution :

depth  $d_a = 104.35247$  m  
 $d_b = 113.04517$  m  
conductivity  $\sigma_a = 0.14044$  S/m  
 $\sigma_b = 5.31054 \cdot 10^{-2}$  S/m  
 $\sigma_{bedrock} = 0.001$  S/m  
cost function 0.22511

The relative errors can be studied in fig (7.6).

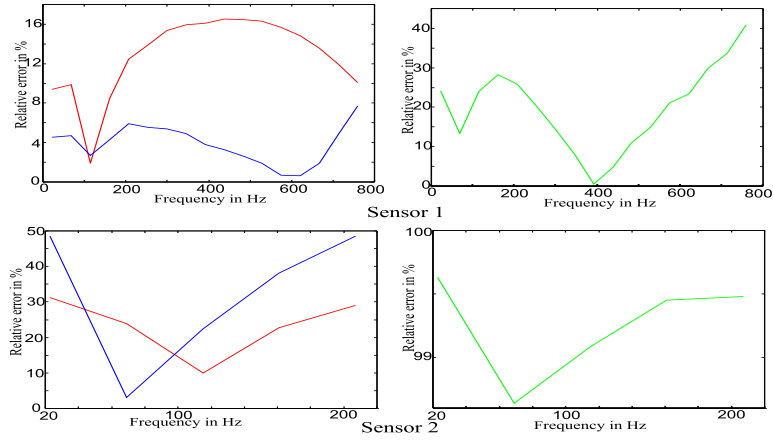


Figure 7.6: Relative errors in the x(red) and y(blue) component at the left and in the z component at the right side. Square wave transmission, five layers.

## Chapter 8

# Conclusions

In this thesis, the INV\_ NLayer\_ RESTART program has been presented. The program has also been used to investigate a number of interesting aspects when trying to find a conductivity profile. When estimating three-layer models, different solutions were presented depending on how much information about the field that was available. From this section we clearly see that knowing the amplitudes of the electric field components gives us a much better result than if we only know the magnitude of the total field. This indicates that it is worth the effort to measure the components. An important thing to mention is that in this investigation we have chosen to measure all three components, even though in chapter two we established that the vertical component in most cases was not important. In the cases where we know that it is not important, only the horizontal components can be used. That gives a better result for these components, but a much worse vertical component. This is a choice the user must do in each case. A summer and a winter case was investigated to try and determine if the sediment and bedrock conductivities needed to be altered with the seasons. Judging from the results in chapter 5, this is not the case. The relative error was larger, but not considerably larger, so other errors are probably a lot bigger than this. Finally, measured data has been analysed with the INV\_ NLayer\_ RESTART program. A three, four and five layer model has been estimated and the relative errors studied. One conclusion drawn from this is that four or five layers seems to be exact enough, since measure errors and above all the model error then dominate.

In fig (8.1) the electric field in sensor 1 in the square-wave case is displayed. The red line describes the measured field, the blue line is the calculated field in the three-layer case, the magenta line is the calculated field in the four-layer case and the green line is the calculated field in the five-layer case. In each step the calculated field improves, but one can see that it improves less in each step.

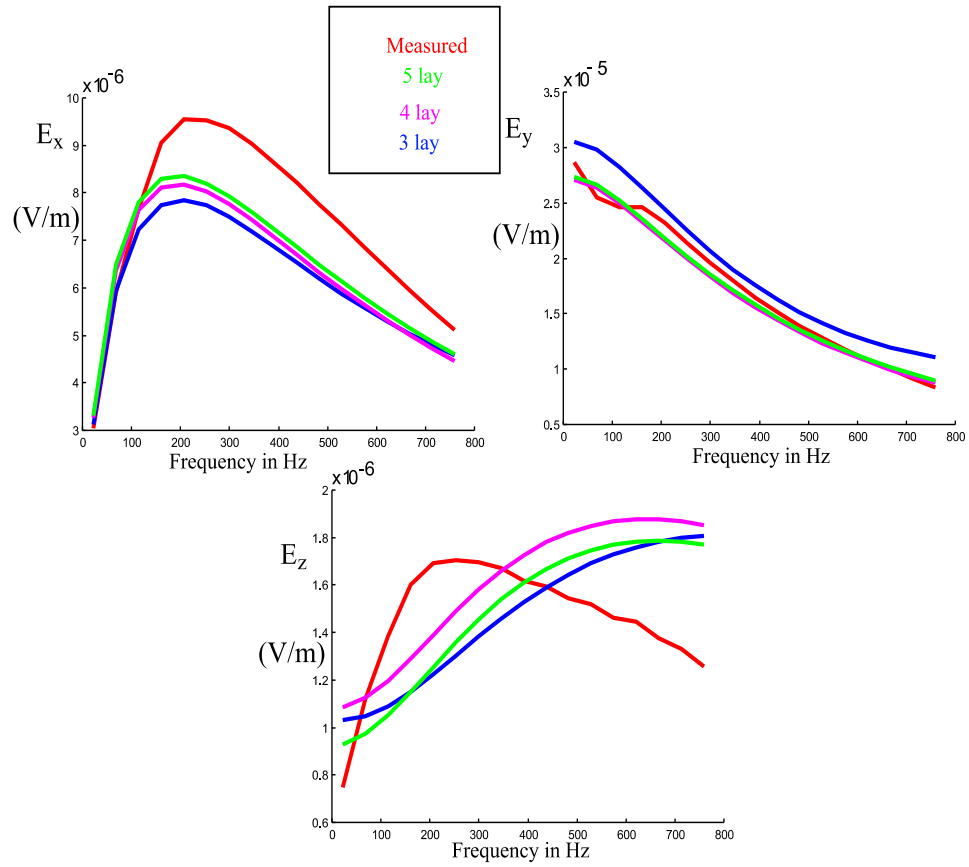


Figure 8.1: Electric field in sensor 1, square wave case. Measured field and calculated field in the three, four and five - layer case.



# List of Figures

2.1	A five-layer model . . . . .	6
5.1	Synthetic winter and summer model . . . . .	13
5.2	A three-layer model . . . . .	14
5.3	The positions of the sensors . . . . .	15
5.4	Relative error in % for the x(red) and y(blue) components. Winter profile, three layers, phase and amplitude information.	16
5.5	Relative error in % for the z component. Winter profile, three layers, phase and amplitude information. . . . .	16
5.6	The cost function . . . . .	17
5.7	Relative errors in the x(red) and y(blue) components. Solu- tion 1 at the left, solution 2 at the right side. Winter profile, three layers, amplitude of the E-field components information.	18
5.8	Relative errors in the z-components. Solution 1 at the left, solution 2 at the right side. Winter profile, three layers, am- plitude of the E-field components information. . . . .	19
5.9	Relative errors in the x(red) and y(blue) components. Winter profile, three layers, total E-field magnitude information. . . .	20
5.10	Relative errors in the z component. Winter profile, three layers, total E-field magnitude information. . . . .	20
5.11	Relative errors in the x(red) and y(blue) components. Sum- mer profile, three layers, phase and amplitude information. . .	21
5.12	Relative errors in the z component. Summer profile, three layers, phase and amplitude information. . . . .	22
5.13	Relative errors in the x(red) and y(blue) components. Solu- tion 1 at the left, solution 2 at the right side. Summer profile, three layers, amplitude of the E-field components information.	23
5.14	Relative errors in the z component. Solution 1 at the left, solution 2 at the right side. Summer profile, three layers, amplitude of the E-field components information. . . . .	24
5.15	Relative errors in the x(red) and y(blue) components. Sum- mer profile, three layers, total E-field magnitude information.	25
5.16	Relative errors in the z component. Summer profile, three layers, total E-field magnitude information. . . . .	25

5.17	A four-layer model. . . . .	26
5.18	Relative errors in the x(red) and y(blue) components. Winter profile, four layers. . . . .	27
5.19	Relative errors in the z component. Winter profile, four layers. . . . .	27
5.20	Relative errors in the x(red) and y(blue) components. Summer profile, four layers. . . . .	28
5.21	Relative errors in the z component. Summer profile, four layers. . . . .	29
5.22	Relative errors in the x and y components. Comparison between summer and winter profiles, three layers. . . . .	30
5.23	Relative errors in the z component. Comparison between summer and winter profiles, three layers. . . . .	30
5.24	Relative errors in the x and y components. Comparison between summer and winter profiles, four layers. . . . .	31
5.25	Relative errors in the z component. Comparison between summer and winter profiles, four layers. . . . .	31
6.1	The trial. . . . .	32
6.2	The cost function for measured data. . . . .	33
6.3	The E-field components in sensor 1. Solution 1 at the left side and solution 2 at the right. Sequence transmission, three layers. . . . .	34
6.4	The E-field components in sensor 2. Solution 1 at the left side and solution 2 at the right. Sequence transmission, three layers. . . . .	35
6.5	The relative errors in the horizontal components. Solution 1 at the left side and solution 2 at the right. Sequence transmission, three layers. . . . .	36
6.6	The relative errors in the vertical component. Solution 1 at the left side and solution 2 at the right. Sequence transmission, three layers. . . . .	36
6.7	The E-field components in sensor 1. Solution 1 at the left side and solution 2 at the right. Sequence transmission, four layers. . . . .	38
6.8	The E-field components in sensor 2. Solution 1 at the left side and solution 2 at the right. Sequence transmission, four layers. . . . .	39
6.9	The relative errors in the horizontal components. Solution 1 at the left side and solution 2 at the right. Sequence transmission, four layers. . . . .	40
6.10	The relative errors in the vertical component. Solution 1 at the left side and solution 2 at the right. Sequence transmission, four layers. . . . .	40
6.11	The relative errors. Square wave transmission, three layers. . . . .	41

6.12	Electric fields in sensor 1 and 2. Red line is measured field, blue line is calculated field. Square wave transmission, three layers. . . . .	42
6.13	The relative errors in the x(red) and y(blue) components at the left side, in the z component at the right. Square wave transmission, four layers. . . . .	43
6.14	Electric field in sensor 1 and 2. Red line is measured field, blue line is calculated field. Square wave transmission, four layers. . . . .	44
7.1	A five-layer model. . . . .	45
7.2	The placement of the depths. . . . .	46
7.3	Relative errors in the x(red) and y(blue) components. Winter profile, five layers. . . . .	47
7.4	Relative errors in the z component. Winter profile, five layers. . . . .	47
7.5	Relative errors in the x(red) and y(blue) component at the left and in the z component at the right side. Sequence transmission, five layers. . . . .	48
7.6	Relative errors in the x(red) and y(blue) component at the left and in the z component at the right side. Square wave transmission, five layers. . . . .	49
8.1	Electric field in sensor 1, square wave case. Measured field and calculated field in the three, four and five - layer case. . .	51

# Bibliography

- [1] Abrahamsson, Leif and Andersson, Brodd Leif, *NLAYER, an ELFE code for horizontally stratified media*, Stockholm: FOA, 1997.
- [2] Cheng, David K., *Field and wave electromagnetics, second edition*, USA: Addison-Wesley Publishing company, Inc, 1989.
- [3] Dennis, J.E, and Schnabel, R.B., *Numerical methods for unconstrained optimisation and non-linear equations*, Eaglewood Cliffs, N.J.: Prentice-Hall, 1983.
- [4] Forssén, Patrik, *User's reference guide for RESTPACK  $\alpha$ -version, Software for testing local optimizers and global optimization*, Stockholm: FOA, 1999.
- [5] Jackson, John David, *Classical electrodynamics, third edition*, USA: John Wiley & sons, Inc., 1999.
- [6] King, Ronold W.P., Owens, Margaret and Wu, Tai Tsun, *Lateral electromagnetic waves: Theory and applications to communications, geophysical exploration, and remote sensing*, USA: Springer Verlag, 1992.
- [7] Krylstedt, Peter and Mattsson, Johan, *INV\_NLAYSCA, a computer program for inverse electromagnetic wave propagation in horizontally stratified dispersive environments*, Stockholm: FOA, 2000.
- [8] Liefvendal, Mattias, *Electromagnetic wave propagation from dipole sources in lossy media*, Stockholm: FOA, 1997.
- [9] Timonov, Alexandre, *Some algorithms and programming codes for the nonlinear least-squares problem via the regularised Newton-Kantorovich method: an application to frequency sounding of a layered medium*, Stockholm: FOA, 2000.